Osteology and phylogeny of Late Jurassic ichthyosaurs from the Slottsmøya Member Lagerstätte (Spitsbergen, Svalbard)

LENE L. DELSETT, AUBREY J. ROBERTS, PATRICK S. DRUCKENMILLER, and JØRN H. HURUM

Phylogenetic relationships within the important ichthyosaur family Ophthalmosauridae are not well established, and more specimens and characters, especially from the postcranial skeleton, are needed. Three ophthalmosaurid specimens from the Tithonian (Late Jurassic) of the Slottsmøya Member Lagerstätte on Spitsbergen, Svalbard, are described. Two of the specimens are new and are referred to *Keilhauia* sp. and Ophthalmosauridae indet. respectively, whereas the third specimen consists of previously undescribed basicranial elements from the holotype of *Cryopterygius kristiansenae*. The species was recently synonymized with the Russian *Undorosaurus gorodischensis*, but despite many similarities, we conclude that there are too many differences, for example in the shape of the stapedial head and the proximal head of the humerus; and too little overlap between specimens, to warrant synonymy on species level. A phylogenetic analysis of Ophthalmosauridae is conducted, including all Slottsmøya Member specimens and new characters. The two proposed ophthalmosaurid clades, Ophthalmosaurinae and Platypterygiinae, are retrieved under some circumstances, but with little support. The synonymy of three taxa from the Slottsmøya Member Lagerstätte with *Arthropterygius* is not supported by the present evidence.

Key words: Ichthyosauria, Ophthalmosauridae, *Undorosaurus*, *Keilhauia*, basicranium, phylogenetic analysis, Jurassic, Norway.

Lene L. Delsett [l.l.delsett@nhm.uio.no], Natural History Museum, P.O. Box 1172 Blindern, 0318 Oslo, Norway; Centre for Ecological and Evolutionary Synthesis, Department of Biosciences, University of Oslo, P.O. Box 1066 Blindern, 0316 Oslo, Norway.
Aubrey J. Roberts [aubrey.roberts@nhm.ac.uk], The Natural History Museum, Earth Sciences, Cromwell Road, London SW7 5BD, UK.
Patrick S. Druckenmiller [psdruckenmiller@alaska.edu], University of Alaska Museum, Fairbanks, Alaska, USA; Department of Geosciences, University of Alaska Fairbanks, Alaska, USA.
Jørn H. Hurum [j.h.hurum@nhm.uio.no], Natural History Museum, P.O. Box 1172 Blindern, 0318 Oslo, Norway.

Introduction

Ichthyosaurs were important marine predators of the Mesozoic seas. With one exception (Fischer et al. 2013a), all Late Jurassic–Cretaceous ichthyosaurs belong to Ophthalmosauridae, a cosmopolitan and speciose clade that has been the subject of considerable interest in the past decade leading to new insights regarding their evolution at the Jurassic–Cretaceous boundary and extinction in the early Late Cretaceous (Fischer et al. 2013a, 2014a, 2016; Fernández and Talevi 2014; Fernández and Campos 2015; Paparella et al. 2016). However, a consensus of relationships within the family remains elusive. While some studies recognize the existence of two major subclades, Ophthalmosaurinae and Platypterygiinae (e.g., Fischer et al. 2012, 2016; Roberts et al. 2014; Delsett et al. 2017), others fail to recover this pattern or find only a monophyletic Platypterygiinae (Maxwell et al. 2015; Paparella et al. 2016; Moon 2017). Understanding ophthalmosaurid phylogeny is critical for interpreting evolutionary rates and ecological diversification of the clade (Fischer et al.
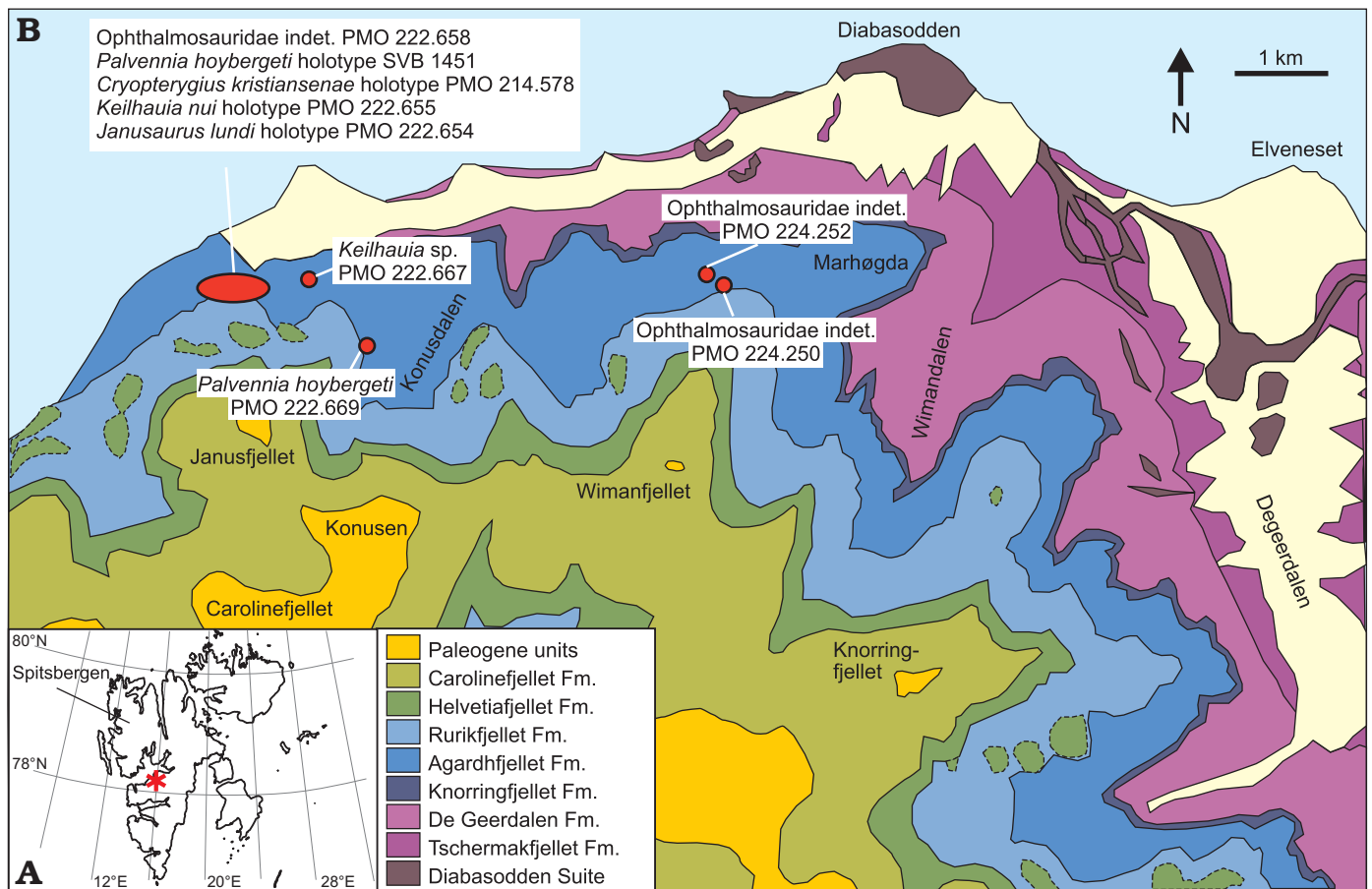
Acta Palaeontol. Pol. 64 (4): 717–743, 2019

https://doi.org/10.4202/app.00571.2018

Fig. 1. **A**. Map of Svalbard archipelago and the main island Spitsbergen with excavation area marked with an asterisk. **B**. Geological map of the excavation sites for the SML ophthalmosaurid specimens described and discussed in this paper (red dots); see Fig. 2. Adapted from Hurum et al. (2012).

2013b, 2016). This requires a better morphological understanding of new and existing specimens from which new and refined cranial and postcranial characters can be based (Maxwell et al. 2015).

The Slottsmøya Member Lagerstätte (SML), Spitsbergen, Norway, contains a diverse assemblage of marine reptiles, particularly plesiosaurians and ichthyosaurs, and provides new data on ophthalmosaurids from at or near the Jurassic/Cretaceous boundary (Hurum et al. 2012; Delsett et al. 2016; Fernández et al. 2018) (Figs. 1, 2). The SML taxa have sometimes been recovered in a monophyletic Ophthalmosaurinae (but see Roberts et al. 2014; Paparella et al. 2016), but many more specimens from this locality remain to be described to further test this phylogenetic hypothesis. Many contemporaneous ichthyosaur specimens to the SML assemblage have been excavated along the Volga River in Russia, which were at the time connected by sea (Mutterlose et al. 2003). Due to problems with accessibility and inadequately published descriptions, many Russian taxa have been reviewed based only on publications and not on personal inspection, and often synonymized with better known taxa from Western Europe (Maisch and Matzke 2000; McGowan and Motani 2003; Maisch 2010) but see Storrs et al. (2000). The only exception is *Undorosaurus* (Efimov 1997, 1999a) which is mostly regarded as valid (Storrs et al. 2000; McGowan and

Motani 2003; Maisch 2010). The Russian specimens are important to the understanding of palaeobiogeography and phylogeny in the Boreal Ocean (Maxwell 2010) and recent publications have provided valuable information (Fischer et al. 2011, 2013b; Zverkov et al. 2015b; Arkhangelsky et al. 2018; Zverkov and Efimov 2019; Zverkov and Prilepskaya 2019).

This paper formally describes three specimens from the Tithonian (Late Jurassic) of the Slottsmøya Member Lagerstätte. PMO 222.667 is referred to *Keilhauia* sp., previously described from the SML and significant for phylogenetic analysis because it preserves a combination of basicranial and pectoral remains. A recent paper assigned newly described ophthalmosaurid specimens from localities in Russia to *Arthropterygius*, and synonymized the SML taxa *Palvennia hoybergeti, Keilhauia nui*, and *Janusaurus lundi* with the genus (Zverkov and Prilepskaya 2019). These taxonomic conclusions are discussed briefly here, while a full evaluation of *Arthropterygius* in Boreal oceans will be addressed thoroughly in a follow-up paper. PMO 224.252 is a skull referred to Ophthalmosauridae indet. The paper also describes basicranial elements from the holotype of *Cryopterygius kristiansenae* (PMO 214.578), one of the most complete and articulated ophthalmosaurids worldwide (Druckenmiller et al. 2012). In 2015, additional mechanical preparation was performed to prepare the specimen for

display, and the basioccipital, a partial basisphenoid and two stapes were removed for description. Similarities between the two genera, *Undorosaurus* and *Cryopterygius*, have been pointed out repeatedly (Druckenmiller et al. 2012; Arkhangelsky and Zverkov 2014; Delsett et al. 2017, 2018) and *Cryopterygius kristiansenae* was recently synonymized with *Undorosaurus gorodischensis* (Zverkov and Efimov 2019). In this contribution, the new interpretations of the holotype of *Cryopterygius kristiansenae* PMO 214.578 by Zverkov and Efimov (2019) are discussed in order to evaluate their hypothesis of synonymy at the species level. A phylogenetic analysis is conducted including all described SML specimens in an expanded matrix using new postcranial characters to investigate their phylogenetic position and discuss interrelationships in Ophthalmosauridae.

Institutional abbreviations.—CAMSM, Sedgwick Museum of Earth Sciences, UK; CMN, Canadian Museum of Nature, Canada; GLAHM, The Hunterian Museum, University of Glasgow, UK; IRSNB, Royal Belgian Institute of Natural Sciences, Brussels, Belgium; LEICT, New Walk Museum and Art Gallery, Leicester, UK; LEIUG, University of Leicester, UK; MANCH, Manchester Museum, UK; MLP, Museo de la Plata, La Plata, Argentina; MOZ, Museo de Paleontología y Mineralogía Prof. Juan F. Olsacher, Zapala, Argentina; NHMUK, Natural History Museum, London, UK; OUMNH, Oxford University Museum, UK; PMO, Natural History Museum, paleontological collections, Oslo, Norway; SNHM Staatliches Naturhistorisches Museum Braunschweig, Germany; SNSB-BSPG, Bayerische Staatssammlung für Paläontologie und Geologie, Munich, Germany; SGS, SVB, Svalbard Museum, Longyear, Spitsbergen; UPM, Paleontological Museum of Undory, Ul'yanovsk, Russia.

Other abbreviations.—CI, consistency index; OTUs, operational taxonomic units; PCA, principal component analysis; RI, retention index; SML, Slottsmøya Member Lagerstätte.

Geological setting

The specimens described herein, PMO 222.667, PMO 224.252, and PMO 214.578 originate from the Late Jurassic–Early Cretaceous Slottsmøya Member Lagerstätte, Spitsbergen, which is the largest island in the Svalbard Archipelago, currently located between 74–81°N and 10–35°E (Fig. 1). During the time of deposition, it was located at 63–66°N (Torsvik et al. 2012). The Lagerstätte spans approximately 12 million years of deposition, is rich in ichthyosaur and plesiosaur skeletons and has an invertebrate fauna comprising ammonites, bivalves, echinoderms, and methane seep communities (Hurum et al. 2012; Rousseau and Nakrem 2012; Hryniewicz et al. 2015; Delsett et al. 2016; Koevoets et al. 2018; Rousseau et al. 2018).

The Slottsmøya Member is part of the Agardhfjellet Formation, Janusfjellet Subgroup, Adventdalen Group. The for-
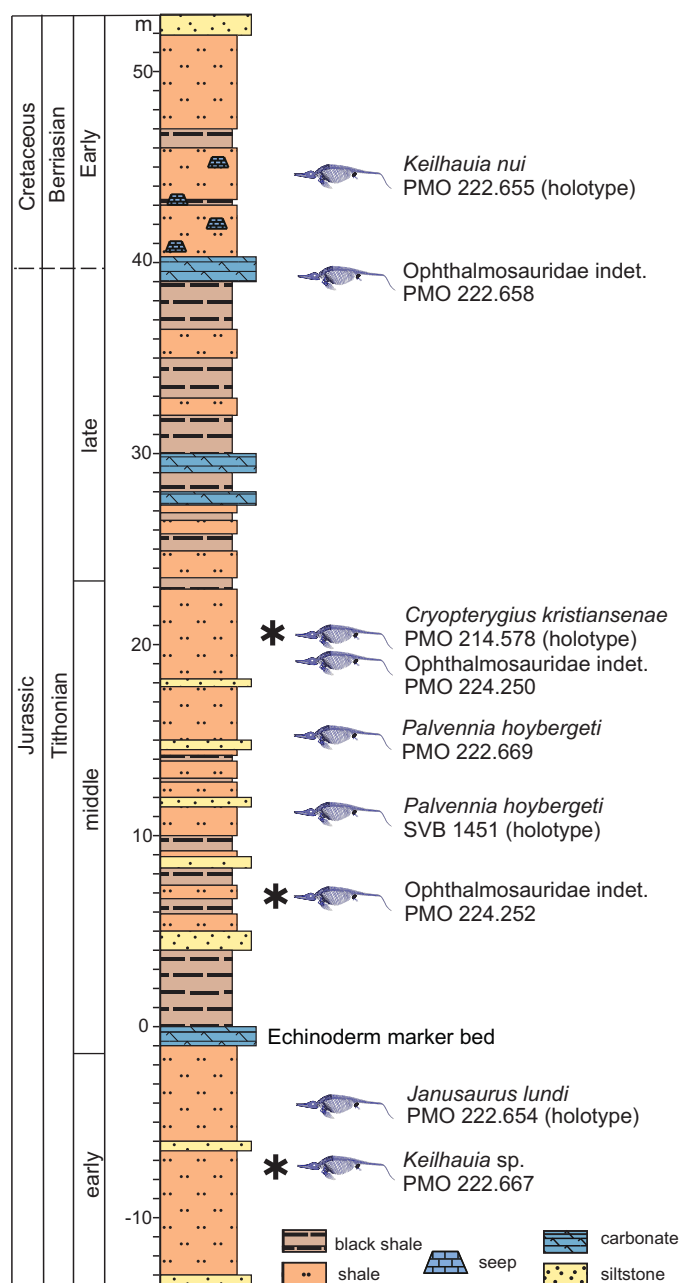

Fig. 2. Composite section of the Slottsmøya Member Lagerstätte with the ophthalmosaurids described and discussed in the text. Specimens described in this paper marked with an asterisk. Modified from Delsett et al. (2017). A bed with a high abundance of echinoderm fossils is set as marker bed (0 m) in the section (Hurum et al. 2012; Rousseau and Nakrem 2012).

mation ranges from the Middle Jurassic (Upper Bathonian) to the earliest Cretaceous (Berriasian) and was deposited in an inner to outer shelf with periodic oxygen-deficient bottom waters (Collignon and Hammer 2012; Koevoets 2017). The lowermost member of the formation is Oppdalen, overlain by Lardyfjellet, Oppdalssåta and Slottsmøya Members. The thickness of the formation varies from 100–250 m (Dypvik and Zakharov 2012; Koevoets et al. 2016). Agardhfjellet Formation mainly consists of black paper shale, grey siltstone, some sandstones and carbonates (Hammer et al. 2012; Koevoets et al. 2016).

The Slottsmøya Member (Fig. 2) was deposited during the Tithonian to earliest Berriasian (Koevoets et al. 2018) and predominantly consists of grey-black shales and siltstone, with interbedded siderites, originating from an offshore transition (Collignon and Hammer 2012; Koevoets et al. 2016, 2018). The member in the studied area is 70–100 meters thick and shows an upwards coarsening trend. The deposition happened under dysoxic conditions with periodic oxygenation (Koevoets et al. 2018).

Material and methods

The taphonomy and stratigraphic position of the specimens is presented in detail in Delsett et al. (2016). The taxa names *Keilhauia nui*, *Janusaurus lundi*, and *Palvennia hoybergeti* are used, as we do not acknowledge their synonymy to *Arthropterygius* based on the evidence presented at the moment (Zverkov and Prilepskaya 2019). The most commonly used chronostratigraphic names (e.g., Tithonian) are used instead of the regional names (Volgian).

The specimens were wrapped in plaster jackets in the field together with surrounding matrix and transported to Natural History Museum in Oslo for preparation using air scribes, air abrasion and manual tools (Roberts et al. 2019). PMO 214.578 was excavated in 2009 and described in 2012 as the holotype of the new genus and species *Cryopterygius kristiansenae* (Druckenmiller et al. 2012). PMO 222.667 was excavated in 2011 and has been mentioned for comparative purposes in two previous papers (Roberts et al. 2014; Delsett et al. 2018). X-ray microtomography was carried out to establish the nature of the teeth in a lower jaw element in PMO 222.667 with a Nikon Metrology XT H 225 ST at the Natural History Museum, Oslo. (µCT scan settings: 195 kV, 220 µA, with a 0.5 mm tin filter and exposure time 1 s. Number of projections: 1606, voxel resolution 70 µm). PMO 224.252 was excavated in 2012. All specimens are housed in the Natural History Museum, University of Oslo. To avoid ambiguities, in the nomenclature of the extracondylar area, Druckenmiller and Maxwell (2013) was followed, which considers all bone surrounding the occipital condyle as extracondylar, regardless of whether it is visible in posterior view or not.

To evaluate interrelationships within Ophthalmosauridae, a phylogenetic analysis was conducted using a modified and extended version of the Fischer et al. (2016) dataset. Eleven operational taxonomic units (OTUs) were added to the matrix: *Paraophthalmosaurus* sp., *Undorosaurus gorodischensis*, *U. nessovi*, *Muiscasaurus catheti*, *Gengasaurus nicosiai*, *Keilhauia nui*, two of the specimens described herein (PMO 222.667 and PMO 224.252) as well as three other specimens referred to Ophthalmosauridae indet. from the same member (PMO 224.250, PMO 222.670, and PMO 222.658) (Arkhangelsky 1997; Efimov 1999a, Maxwell et al. 2015, Paparella et al. 2016; Delsett et al. 2017; Delsett et al. 2018; SOM 1, 2, Supplementary Online Material available at http://app.pan.pl/SOM/app64-Delsett_etal_SOM.pdf).

Two characters (48 and 56) were modified to accommodate variations in rib cross section in SML specimens and to more precisely separate features of the acromion process on the scapula, respectively. Sixteen characters in the basicranium and postcranium were added based on Moon (2017) and Maxwell et al. (2015) because these were judged to account for variation within Ophthalmosauridae (SOM 1.1). An additional six new characters (SOM 1.1) were added based on observations of variation in the parietal foramen, basicranium, pectoral and pelvic girdles in SML specimens (Druckenmiller et al. 2012; Roberts et al. 2014; Delsett et al. 2017, 2018). In total, the most inclusive dataset included 47 OTUs and 110 characters (analysis 1).

The analyses was run in TNT 1.5 (Goloboff and Catalano 2016), with a traditional search, 20 000 trees in memory, TBR, 1000 replications and 10 trees saved per replication. Bremer support was calculated using the bremer script. In a second run of the analysis, taxa that were scored for less than 25% of the characters were pruned (Fischer et al. 2014b; Maxwell et al. 2015). This excluded *Malawania anachronus*, *Mollesaurus periallus*, *Leninia stellans*, *Simbirskiasaurus birjukovi*, *Pervushovisaurus bannovkensis*, *Muiscasaurus catheti*, PMO 224.252, PMO 222.658, and PMO 222.670. To investigate the influence of the new characters added in this study, the matrix was also analysed excluding these characters, one iteration including and another excluding the pruned taxa listed above (analysis 3 and 4, SOM 2.1).

Systematic palaeontology

Ichthyosauria de Blainville, 1835

Neoichthyosauria Sander, 2000

Thunnosauria Motani, 1999

Ophthalmosauridae Baur, 1887

Genus *Keilhauia* Delsett, Roberts, Druckenmiller, and Hurum, 2017

Type species: *Keilhauia nui*, Slottsmøya Member Lagerstätte, Spitsbergen, Svalbard (Berriasian).

Keilhauia sp.

Material.—PMO 222.667 (Figs. 3–7, SOM 4: table 1), a partially articulated anterior portion of a skeleton. The carcass landed ventrally on the sea floor, and the elements are three-dimensional with few signs of distortion and compression compared to many other specimens from the same unit (Delsett et al. 2016). The skull suffered a collapse during excavation. Approximately 50 incomplete teeth, two partial quadrates, a basioccipital and a basisphenoid, both articulars and a partial stapes were preserved disarticulated, as well as two partial hyoids. The atlas-axis and 23 additional vertebrae are preserved, with 15 neural arches, 35 ribs and several broken gastralia. Seventeen of the vertebrae are articulated with neural arches and with the gastralia,
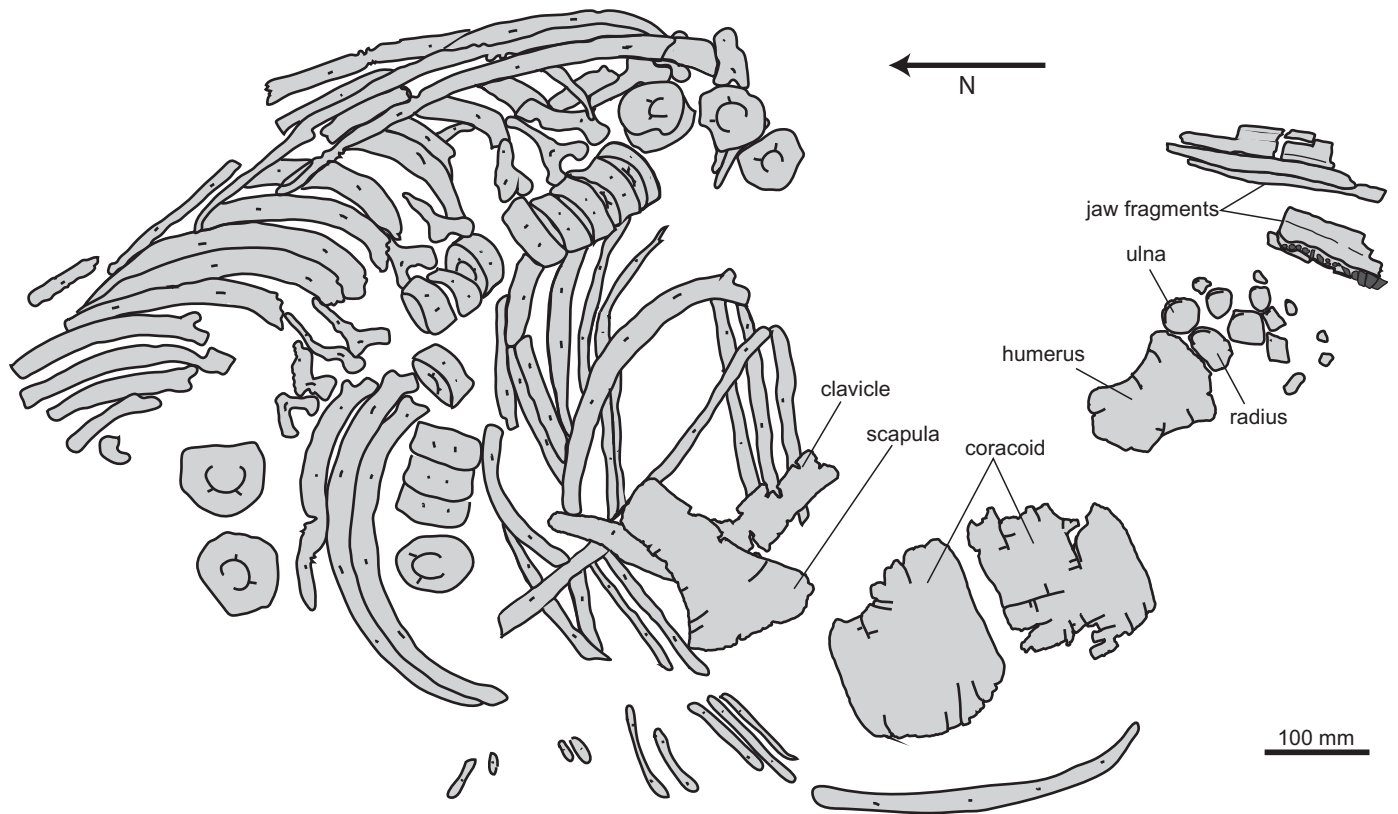
Fig. 3. Explanatory drawing of the skeleton of ophthalmosaurid ichthyosaur *Keilhauia* sp. (PMO 222.667) from Spitsbergen, Svalbard, Slottsmøya Member Lagerstätte, Tithonian. Modified and corrected from Delsett et al. (2016).

while the atlas-axis and four vertebrae were found in the proximity. Both scapulae are preserved, but only the left is complete. A partial interclavicle and two partial clavicles are preserved, in addition to one complete and one incomplete coracoid and the right humerus, which is preserved with 24 epi- and autapodial elements.

Description.—Premaxilla, nasal, and vomer (Fig. 4A): The preserved portion of the upper rostrum in PMO 222.667 (*Keilhauia* sp.) consists of partial premaxillae, nasals and vomers. The elements lack the anterior- and posteriormost ends and are fractured, but three-dimensional with surface details preserved. The premaxilla has the typical longitudinal groove dorsal to the alveolar groove as in many ophthalmosaurids such as *Ophthalmosaurus icenicus* (Moon and Kirton 2016) and *Platypterygius australis* (Kear 2005), but the groove is deeper in *Undorosaurus? kristiansenae* (Druckenmiller et al. 2012). The alveolar groove is shallow and lacks tooth impressions. In anterior view the anterior elongated portion of the nasals have a triangular cross section with a flattened ventral margin. They are visible in dorsal view between the two premaxillae and decrease in dorsoventral height posteriorly. The anterior portions of the vomers are shifted laterally towards the left side of the rostrum. They are oval in cross section and increase in dorsoventral height posteriorly.

Basioccipital (Fig. 5A): The basioccipital of PMO 222.667 (*Keilhauia* sp.) is complete and three-dimensional, with only a few fractures. The anteroposterior length of the basioccipital is approximately the same as the dorsoventral height in lateral view, whereas in *Janusaurus lundi* the element is anteroposteriorly longer than tall (Roberts et al. 2014). In dorsal view, the element is mediolaterally wider than anteroposteriorly long, as *Gengasaurus nicosiai* (Paparella et al. 2016) and *Ophthalmosaurus icenicus* (Moon and Kirton 2016). Most of the anteroventral surface of the basioccipital (Fig. 5A$_6$) articulated with the basisphenoid and bears a shallow dorsoventrally oriented notochordal groove, as in *Arthropterygius chrisorum* (Maxwell 2010) and *Ophthalmosaurus icenicus* (Moon and Kirton 2016), whereas a groove is absent in *Simbirskiasaurus birjukovi* (Fischer et al. 2014b) and *Palvennia hoybergeti* (Druckenmiller et al. 2012; Delsett et al. 2018). Dorsally, the groove terminates in a notochordal pit, similar to *Platypterygius australis* (Kear 2005). The specimen lacks a basioccipital peg as *Palvennia hoybergeti* (Druckenmiller et al. 2012) and *Platypterygius hercynicus* (Kolb and Sander 2009), whereas this feature is variably present in *Ophthalmosaurus icenicus* (Moon and Kirton 2016).

The occipital condyle (Fig. 5A$_1$) is approximately circular in posterior view as in *Arthropterygius chrisorum* (Maxwell 2010) and *Acamptonectes densus* (Fischer et al. 2012), whereas it is mediolaterally wider than tall in *Janusaurus lundi* (Roberts et al. 2014) and *Palvennia hoybergeti* (Druckenmiller et al. 2012). The surface of the condyle is smooth. The notochordal pit is eight-shaped and situated near the middle of the condyle as in the SML
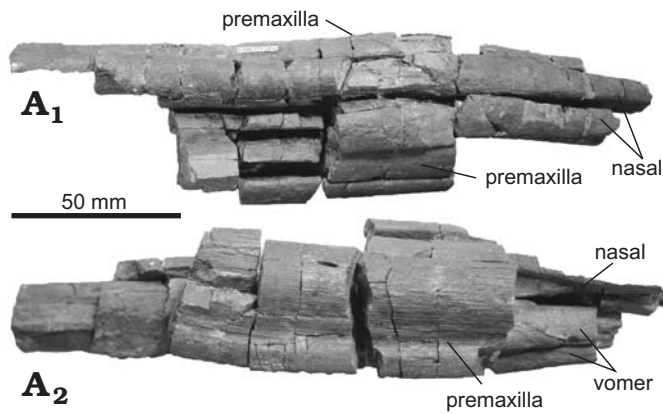
Fig. 4. Rostrum fragment of ophthalmosaurid ichthyosaur *Keilhauia* sp. (PMO 222.667) from Spitsbergen, Svalbard, Slottsmøya Member Lagerstätte, Tithonian. Premaxillae, nasals, and vomer in dorsal (A_1) and lateral (A_2) views. Anterior to the right.
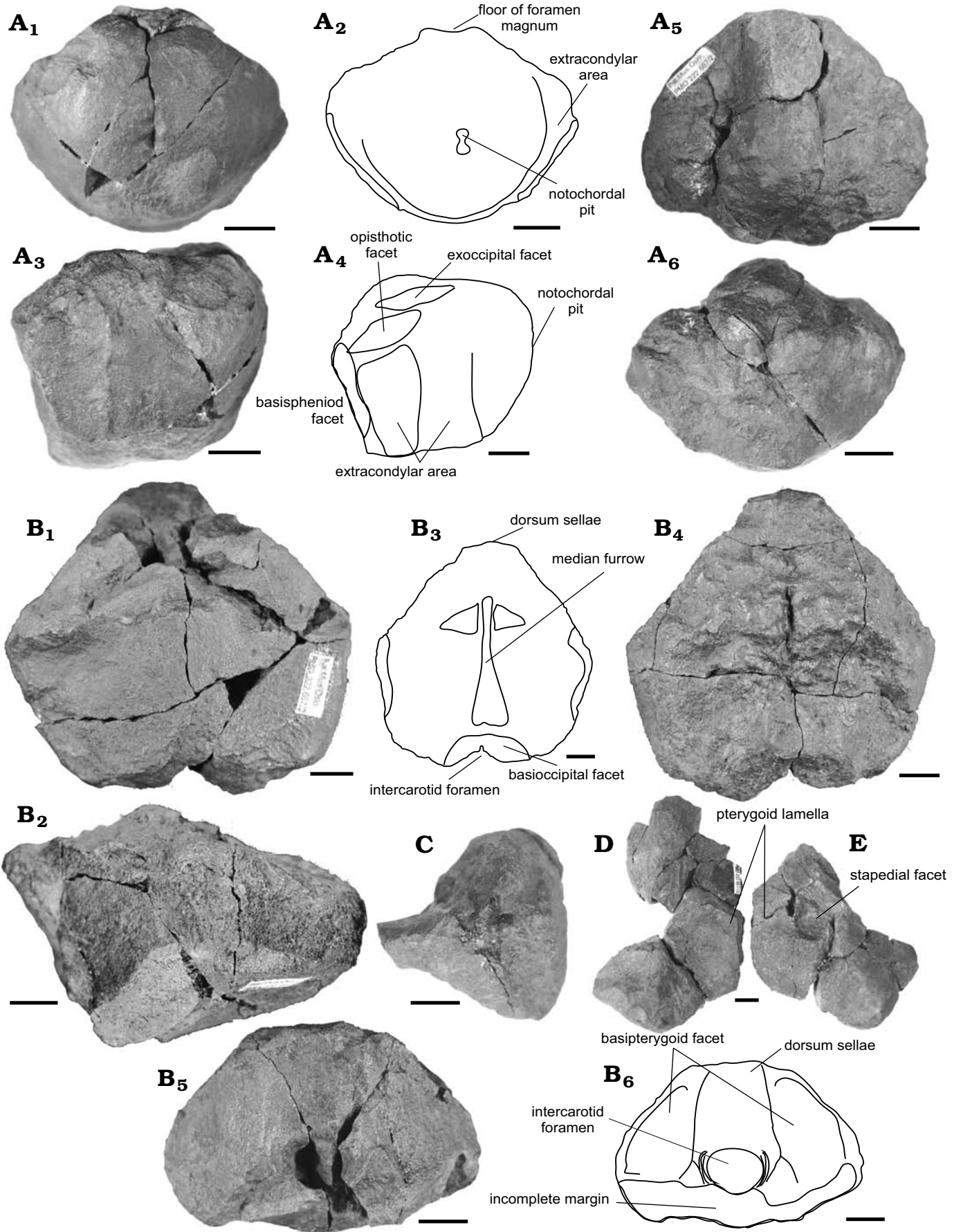
Ophthalmosauridae indet. specimen PMO 224.250 (Delsett et al. 2018). The condyle is poorly demarcated in posterior view and only a small portion of the extracondylar area is visible, as in *Brachypterygius extremus*, *Muiscasaurus catheti*, *Sveltonectes insolitus*, *Janusaurus lundi*, and "*Grendelius*" *alekseevi* (McGowan 1976; Fischer et al. 2011; Roberts et al. 2014; Maxwell et al. 2015; Zverkov et al. 2015a). In *Palvennia hoybergeti* (Druckenmiller et al. 2012) and *Simbirskiasaurus birjukovi*, no extracondylar area is visible in posterior view (Fischer et al. 2014b), whereas a large portion is visible in *Ophthalmosaurus icenicus* (Moon and Kirton 2016), *Undorosaurus? kristiansenae* (see description of this element below) and *Leninia stellans* (Fischer et al. 2013b). The extracondylar area immediately surrounding the condyle laterally (Fig. $5A_3$) and ventrally consists of unfinished bone, and anterior to this is an area of finished bone on each lateral surface that do not meet ventrally, as in *Palvennia hoybergeti* (Delsett et al. 2018). The floor of the foramen magnum (Fig. $5A_5$) is elevated and bears a shallow groove on the dorsal surface. The exoccipital facets are less prominent than in *Sisteronia seeleyi* (Fischer et al. 2014a) and *Mollesaurus periallus* (Fernández 1999). The opisthotic facets are raised as in *Palvennia hoybergeti* and *Sveltonectes insolitus* (Fischer et al. 2011; Delsett et al. 2018), in contrast to *Simbirskiasaurus birjukovi* (Fischer et al. 2014b); but they are not dorsoventrally elongated, in contrast to *P. hoybergeti* (Delsett et al. 2018). The ventral surface of the basioccipital is convex. It lacks a ventral notch, as many other ophthalmosaurids (e.g., Druckenmiller et al. 2012; Fischer et al. 2014a; Roberts et al. 2014), in contrast to *Ophthalmosaurus icenicus* (Moon and Kirton 2016).

Basisphenoid (Fig. 5B): The basisphenoid of PMO 222.667 (*Keilhauia* sp.) is three-dimensional, with a ventral and anterior surface missing some parts. It differs from

most other ophthalmosaurids in overall shape. We interpret the rugose and pentagonal surface as dorsal (Fig. $5B_4$) because it has a median furrow, whereas the ventral surface is flat and smooth (following McGowan 1976; Fischer et al. 2011; Moon and Kirton 2016). The foramina for the carotid are thus situated on the anterior and posterior surfaces. On the dorsal surface, one third of the anteroposterior distance from the anterior margin is a dorsally tall ridge on each side of the furrow representing the anterior margin of the basioccipital facet, which extends to the posterior margin of the element. The dorsal surface (Fig. $5B_4$) is strikingly similar to the posterior surface of the basisphenoid in *Acamptonectes densus* (Fischer et al. 2012) in having a pentagonal shape with a middle furrow for most of its length. In our preferred orientation, the apex of the pentagon in dorsal view is directed anteriorly and represents the dorsum sellae, based on similarity to *Ophthalmosaurus icenicus* (Moon and Kirton 2016). This contrasts the interpretation of the basisphenoid in *Acamptonectes densus*, which implies that the basioccipital has a dorsal crest instead of a flattened dorsal surface (Fischer et al. 2012). As in *Ophthalmosaurus icenicus*, PMO 222.667 has a large carotid foramen in the middle of the anterior surface (Fig. $5B_5$, B_6), with the dorsum sellae overhanging the opening in anterior view (Moon and Kirton 2016). On each side of the carotid foramen are facets probably for articulation to the pterygoids. In ventral view the articulation for the basipterygoid do not form processes as in other ophthalmosaurids, which means that they are smaller than the reduced processes in *Sveltonectes insolitus* and *Sisteronia seeleyi* (McGowan 1976; Fischer et al. 2011, 2014a; Moon and Kirton 2016; Delsett et al. 2018). The parasphenoid probably originated ventral to the anterior carotid foramen as in e.g., *Platypterygius australis* and *Sisteronia seeleyi* (Kear 2005; Fischer et al. 2014a), but this area is incomplete. The carotid exits posteriorly as in *Arthropterygius chrisorum* (Maxwell 2010) and *Palvennia hoybergeti* (Delsett et al. 2018), in contrast to other ophthalmosaurids where it exits ventrally (McGowan 1976; Fernández 1999; Maxwell and Caldwell 2006; Fischer et al. 2011, 2014a; Moon and Kirton 2016). In *Platypterygius australis* the carotid arteries run from the anterodorsal to the posteroventral surfaces (Kear 2005).

Stapes (Fig. 5C): The preserved portion of the stapes of PMO 222.667 (*Keilhauia* sp.) is the medial head as well as a minor portion of the shaft. The medial head has a smooth surface interpreted as the posterior surface. Compared to the shaft, the medial head is more dorsoventrally expanded in one direction, and based on its similarity to *Palvennia hoybergeti* (Delsett et al. 2018), it is interpreted to be the dorsal portion. Following from this, the element is the right stapes. The medial head is roughly triangular in medial view with a dorsal,

Fig. 5. Basicranium elements of ophthalmosaurid ichthyosaur *Keilhauia* sp. (PMO 222.667) from Spitsbergen, Svalbard, Slottsmøya Member Lagerstätte, → Tithonian. **A**. Basioccipital in posterior (A_1, A_2), left lateral (A_3, A_4), dorsal (A_5), and anterior (A_6) views. **B**. Basisphenoid in ventral (B_1), left lateral (B_2), dorsal (B_3, B_4), and anterior (B_5, B_6) views. **C**. Medial head of stapes in posterior view. **D**. Left quadrate in posterior view. **E**. Right quadrate in posterior view. Photographs (A_1, A_3, A_5, A_6, B_1, B_2, B_4, B_6, C–E) and interpretative drawings (A_2, A_4, B_3, B_5). Scale bars 10 mm.

A₁

A₂

floor of foramen magnum
extracondylar area
notochordal pit

A₅

A₃

A₄

opisthotic facet
exoccipital facet
notochordal pit
basispheniod facet
extracondylar area

A₆

B₁

B₃

dorsum sellae
median furrow
intercarotid foramen
basioccipital facet

B₄

B₂

C

D

pterygoid lamella

E

stapedial facet

B₅

B₆

basipterygoid facet
dorsum sellae
intercarotid foramen
incomplete margin

triangular opisthotic facet. A ridge runs dorsoventrally across the medial surface and represents the posterior margin of the facet for the basioccipital, which is more well-defined than in *Palvennia hoybergeti* (Druckenmiller et al. 2012; Delsett et al. 2018). Ventral and anterior to the basioccipital facet is the facet for the basisphenoid. The preserved portion of the shaft has a dorsoventrally narrower posterior than anterior margin, resulting in a pyriform cross section as in *Platypterygius australis* (Kear 2005). The shaft is slender in posterior view as in *Janusaurus lundi* and *Palvennia hoybergeti*, and narrower than in *Ophthalmosaurus icenicus, Acamptonectes densus* and *Undorosaurus*? *kristiansenae* (Druckenmiller et al. 2012; Fischer et al. 2012; Roberts et al. 2014; Moon and Kirton 2016; Delsett et al. 2018). The disarticulated piece interpreted as the lateral head resembles that of *Janusaurus lundi* (Roberts et al. 2014) in being dorsoventrally and anteroposteriorly narrow compared to the more robust lateral head of *Undorosaurus*? *kristiansenae* (see description of this element below).

Quadrate (Fig. 5D, E): The quadrates of PMO 222.667 (*Keilhauia* sp.) are oriented based on *Ophthalmosaurus icenicus* (Moon and Kirton 2016). The left quadrate is the most complete, but is missing dorsal and lateral portions of the occipital lamella. The element lacks a dorsoventral ridge separating it into defined occipital and pterygoid lamellae, which is found in the Ophthalmosaurinae indet. specimen UAMES 34111 (Druckenmiller and Maxwell 2013). In posterior view, the medial margin of the pterygoid lamella is straighter than the more convex outline in *Palvennia hoybergeti* and *Acamptonectes densus* (Fischer et al. 2012; Delsett et al. 2018). The medial margin of the pterygoid lamella bears a dorsoventrally oriented groove interpreted as the facet for the supratemporal. The shallow stapedial facet has a thickened ventral margin, as is common in ophthalmosaurids, e.g., *Acamptonectes densus* (Fischer et al. 2012) and *Sisteronia seeleyi* (Fischer et al. 2014a). In ventral view, the articular condyle is rhomboid and mediolaterally wider than anteroposteriorly long, as the Ophthalmosaurinae indet. specimen UAMES 3411 (Druckenmiller and Maxwell 2013). The articular condyle bears two facets separated by a shallow mediolaterally oriented groove, similar to *Sveltonectes insolitus* (Fischer et al. 2011) and *Ophthalmosaurus icenicus*. The posterior and triangular facet is interpreted to be the articular facet and is the largest, while the mediolaterally elongated anterior facet is for articulation with the surangular (Druckenmiller and Maxwell 2013; Moon and Kirton 2016).

Lower jaw (Fig. 6A$_1$, A$_2$): Only a small portion of what is interpreted as the right dentary is preserved, with an intact tooth row. Medially to the teeth is a narrow element that probably represents the dorsal anterior process of the splenial.

Articular (Fig. 6B): The articular of PMO 222.667 (*Keilhauia* sp.) is complete and interpreted to be a right articular based on its similarity to those of *Palvennia hoybergeti* and *Platypterygius australis* (Kear 2005; Delsett et al. 2018).

The element is mediolaterally compressed, similar to most other ophthalmosaurids but unlike *Acamptonectes densus* (Fischer 2012). In anterior view, the articular surface is oval and not triangular as in *Palvennia hoybergeti* (Delsett et al. 2018). In medial view (Fig. 6B$_1$); the dorsal margin is slightly convex in contrast to the concave margin of *Palvennia hoybergeti*, but less convex than in *Platypterygius australis* (Kear 2005; Delsett et al. 2018). The medial surface is convex, decreasing in mediolateral thickness into a thin flange on the ventral surface in the posterior half of the element, with a longer ventral reach than in *Palvennia hoybergeti* (Delsett et al. 2018). The articular of *Sisteronia seeleyi* has a similar medial surface but lacks the ventral flange (Fischer et al. 2014a). The lateral surface (Fig. 6B$_2$) is flat and featureless except for a small diagonal ridge, similar to but less well-defined than in *Mollesaurus periallus* (Fernández 1999; personal observations AJR on MOZ 2282 V). The posterior margin is mediolaterally thickened in comparison to the middle of the element, in contrast to *Palvennia hoybergeti* (Delsett et al. 2018).

Dentition (Fig. 6D–F): Some teeth are still attached to the dentary in PMO 222.667 (*Keilhauia* sp.) (Fig. 6A$_2$, A$_3$) and are tightly packed as in *Aegirosaurus leptospondylus* (Bardet and Fernández 2000; personal observations LLD on SNSB-BSPG1954 I 608). As preserved, they are posteriorly inclined. In the posterior portion are two rows of teeth adjacent to each other. µCT scan showed that the apex of the crowns belonging to one tooth row are ventrally directed and are interpreted as belonging to the dentary (Fig. 6A$_2$, A$_3$). None of the teeth are preserved in entirety, but based on the remains; none of them seem to have surpassed 30 mm in total length (crown + root). The crown is slightly curved (Fig. 6D) as in *Aegirosaurus leptospondylus* (Bardet and Fernández 2000; personal observations LLD on SNSB-BSPG1954 I 608) and *Platypterygius australis* (Kear 2005). The crown is finely striated with parallel striations that extend from the base of the crown to the tip (Fig. 6D–F), as in *Platypterygius australis* (Kear 2005) and *Athabascasaurus bitumineus* (Druckenmiller and Maxwell 2010). The base of the enamel is well defined and forms a straight line, as in *Pervushovisaurus bannovkensis* (Fischer et al. 2014b) and *Paraophthalmosaurus* (Efimov 1999b), but the crown is not as narrow compared to the root as in *Paraophthalmosaurus* (Efimov 1999b), nor has it a constriction at the base, as in *Acamptonectes densus* (Fischer et al. 2012). In cross section, the root is rounded, as in *Undorosaurus*? *kristiansenae* and *Keilhauia nui* (Druckenmiller et al. 2012; Delsett et al. 2017), but in contrast to *Palvennia hoybergeti* (Delsett et al. 2018). A single root is squared in cross section, but this seems to be due to erosion or resorption. In *Ophthalmosaurus icenicus,* the roots are transversely compressed (Moon and Kirton 2016), but this is not seen in PMO 222.667. Quadrangular roots are found in several ophthalmosaurids e.g., *Acamptonectes densus* (Fischer et al. 2012) and *Sisteronia seeleyi* (Fischer et al. 2014a). Unlike
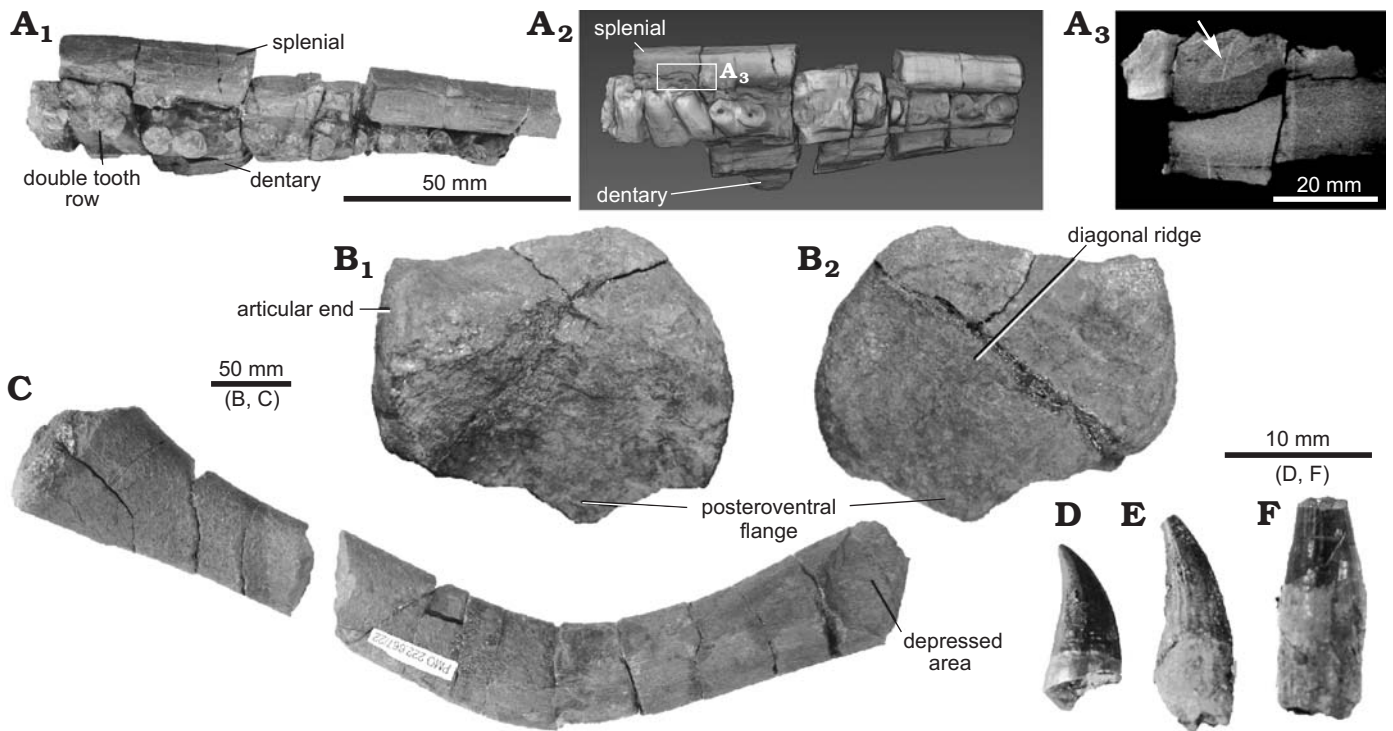
Fig. 6. Cranial elements of ophthalmosaurid ichthyosaur *Keilhauia* sp. (PMO 222.667) from Spitsbergen, Svalbard, Slottsmøya Member Lagerstätte, Tithonian. **A**. Lower jaw fragment in dorsal view (anterior to the left). A_3, detail of inner structures with arrow showing position of ventral-pointing tooth from the upper jaw, anterior to the right, in dorsal view. **B**. Right articular in medial (B_1) and lateral (B_2) views. **C**. Hyoid in lateral or medial view (anterior to the left). **D–F**. Teeth. Photographs (A_1, B–F), μCT scan images (A_2, A_3).

Simbirskiasaurus birjukovi, the teeth lack apicobasal ridges in the root (Fischer et al. 2014b).

Hyoid (Fig. 6C): Two partial hyoids from of PMO 222.667 (*Keilhauia* sp.) are preserved; one is in pieces, while the second consists of two larger portions that likely belong to the same element. The hyoid is more strongly curved than *Platypterygius hercynicus* (Kolb and Sander 2009), *P. australis* (Kear 2005), *Janusaurus lundi* (Roberts et al. 2014) and *Palvennia hoybergeti* (Delsett et al. 2018). The element has an oval cross section, and is more flattened at the end interpreted to be anterior than the posterior, as in *Platypterygius hercynicus* (Kolb and Sander 2009) and *Gengasaurus nicosiai* (Paparella et al. 2016). In anterior view, the anterior end is mediolaterally narrow and pitted. The posterior portion has a depression on both sides as in *Palvennia hoybergeti* (Delsett et al. 2018)

Interclavicle (Fig. 7A): The interclavicle of PMO 222.667 (*Keilhauia* sp.) has the T-shape in ventral view (Fig. $7A_1$) typical of ophthalmosaurids, with incomplete lateral and posterior margins. The element is dorsoventrally thin and fused to the medial portions of the two clavicles with a visible suture (Fig. $7A_2$), a feature found in some of the largest and presumably more mature *Ophthalmosaurus icenicus* specimens (Moon and Kirton 2016). The dorsal surface of the element is flat and makes a 90° angle to the medial portions of the clavicles (Fig. $7A_3$). In ventral view, the transverse bar is relatively tall compared to the width, in contrast to the narrower transverse bar in *Ophthalmosaurus icenicus* and

Undorosaurus? *kristiansenae* (Druckenmiller et al. 2012; Moon and Kirton 2016). The ventral surface of the transverse bar is rugose, but lacks the triangular structure found in *Caypullisaurus bonapartei* (personal observations AJR on MLP 83-XI-16-1). The transition posteriorly to the median stem is gradual, as in *Janusaurus lundi* (Roberts et al. 2014) and *Paraophthalmosaurus* (Efimov 1999b, personal observations LLD on UPM EP-II-7[1235]), in contrast to *Undorosaurus*? *kristiansenae* where the transition between the two parts is more abrupt (Druckenmiller et al. 2012).

Clavicle (Fig. 7B): The preserved left clavicle is fractured, but almost complete, only missing some pieces in the medial portion. As in the holotype of *Keilhauia nui*, the clavicles in PMO 222.667 have dorsoventrally narrow medial ends without the interdigitating margin often found in ophthalmosaurids (Moon and Kirton 2016; Delsett et al. 2017), but in PMO 222.667 the medial portion is thicker than in *K. nui*. The anteroposterior length of the medial portion of the clavicle is less than in *Paraophthalmosaurus* (personal observations LLD on UPM EP-II-7[1235]). The curvature between the anterior and posterior portions is approximately similar to *Aegirosaurus leptospondylus* (Bardet and Fernández 2000) and some specimens of *Ophthalmosaurus icenicus* (personal observations LLD on CAMSM J68689) but more curved than in other *O. icenicus* specimens (personal observations LLD on LEIUG 90986). The facet for the scapula on the posterior portion is demarcated by a ridge running along the anterior margin on the ventral surface.
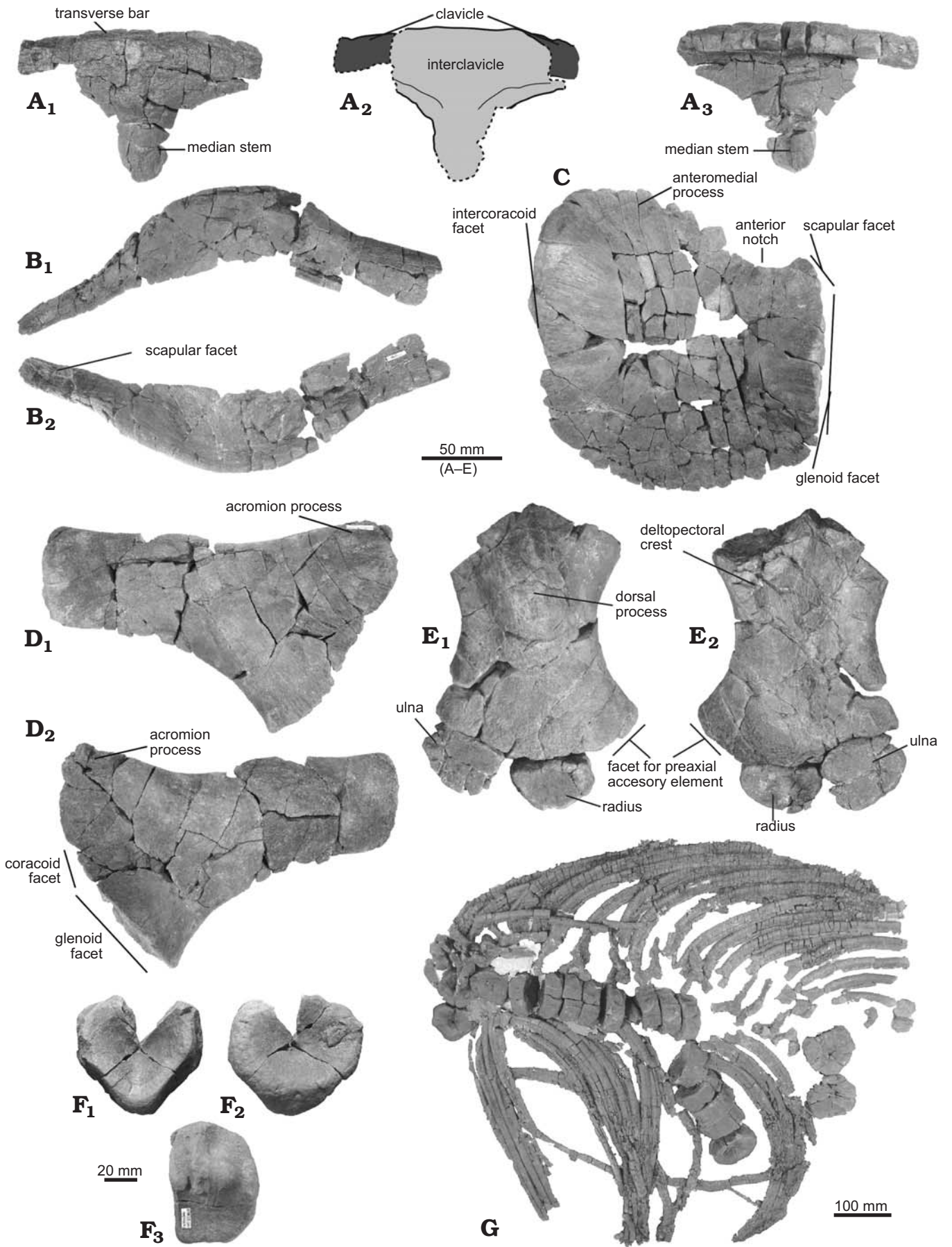
Coracoid (Fig. 7C): PMO 222.667 (*Keilhauia* sp.) preserves a complete left and an incomplete right coracoid. The elements are three-dimensional but fractured. The element is anteroposteriorly longer than mediolaterally wide, similar to the holotype of *Keilhauia nui* and *Undorosaurus*? *kristiansenae* (Druckenmiller et al. 2012; Delsett et al. 2017); but it is not as mediolaterally narrow as *Paraophthalmosaurus* (UPM EP-II-7[1235], personal observations LLD) (Arkhangelsky 1997; Efimov 1999b). Due to the almost straight lateral and medial margins, the outline of the coracoid is more square than *Acamptonectes densus* (Fischer et al. 2012), and more similar to some *Ophthalmosaurus icenicus* specimens (e.g., CAMSM J65813 and LEICT 100 1949 2, personal observations LLD). As preserved, the anterior notch is mediolaterally wider and anteroposteriorly shallower than in *Keilhauia nui* (Delsett et al. 2017) and *Janusaurus lundi* (Roberts et al. 2014). Compared to *Janusaurus lundi* (Roberts et al. 2014), the coracoid of PMO 222.667 has dorsoventrally taller glenoid and intercoracoid facets, giving the ventral surface of the coracoid a pronounced saddle-shape, whereas the dorsal surface is flat. The glenoid and scapular facets are rugose and not well demarcated, similar to *Acamptonectes densus* (Fischer et al. 2012) but in contrast to *Sveltonectes insolitus* (Fischer et al. 2011), and less than in the holotype of *Keilhauia nui* (Delsett et al. 2017). There is less of an angle between the two facets than in *Arthropterygius chrisorum* (Maxwell 2010) and *Platypterygius hercynicus* (Kolb and Sander 2009), and the scapular facet is the smaller. Similar to *Arthropterygius chrisorum* (Maxwell 2010), the intercoracoid facet runs along the entire anteroposterior length of the coracoid, in contrast to *Undorosaurus*? *kristiansenae* where it covers only the anterior half (Druckenmiller et al. 2012). The facet is pyriform in medial view and tallest anteriorly. The posterior margin of the coracoid is gently convex in dorsal view and dorsoventrally thin, with a groove running along the entire margin in posterior view, which is not found in *Acamptonectes densus* (Fischer et al. 2012).

Scapula (Fig. 7D): The left scapula of PMO 222.667 (*Keilhauia* sp.) is complete, whereas the right is incomplete, but both of them are three-dimensionally preserved. The scapula has a dorsoventrally expanded anterior portion and a straight posterior shaft. In lateral view, the anterior portion is less evenly dorsally and ventrally expanded than in *Platypterygius australis* and *P. americanus* (Maxwell and Kear 2010; Zammit et al. 2010). PMO 222.667 resembles *Keilhauia nui* in having a slightly emarginated dorsal margin producing an acromion process that is less dorsally prominent than in *Sveltonectes insolitus* (Fischer et al. 2011) and *Acamptonectes densus* (Fischer et al. 2012) but larger than in *Undorosaurus*? *kristiansenae* (Druckenmiller et al.

2012). The dorsolateral flange is small as in *Keilhauia nui* (Delsett et al. 2017). Ventral to the acromion process, the anterior margin is mediolaterally narrow and widens ventrally to form the coracoid and glenoid facets, which are poorly demarcated. The glenoid facet is oval in anterior view, coarsely rugose and slightly less than twice the dorsoventral height of the coracoid facet as in *Acamptonectes densus* (Fischer et al. 2012). In *Undorosaurus*? *kristiansenae* (Druckenmiller et al. 2012) the two facets are more similar in height. The shaft is mediolaterally compressed as in *Keilhauia nui* and *Acamptonectes densus* (Fischer et al. 2012; Delsett et al. 2017) in contrast to the rounded cross section in *Platypterygius hercynicus* (Kolb and Sander 2009). The posterior shaft has approximately the same dorsoventral height for all of its proximodistal length, in contrast to most ophthalmosaurids where the distalmost margin is dorsoventrally expanded in lateral view (e.g., Zammit et al. 2010; Fischer et al. 2011; Druckenmiller et al. 2012). As in *K. nui*, the distal end is angled so that the dorsal margin runs further posteriorly than the ventral margin (Delsett et al. 2017).

Humerus (Fig. 7E): One humerus of PMO 222.667 (*Keilhauia* sp.) is complete and well preserved, and interpreted as a right humerus based on McGowan and Motani (2003) because of the anteriorly directed, larger and more "plate-like" process interpreted as the dorsal process. The proximal surface is relatively flat, with a low ridge along the articular facet and is slightly dorsoventrally taller than the distal, as in *Janusaurus lundi* (Roberts et al. 2014). The dorsal process (Fig. 7E$_1$) is larger than the deltopectoral crest (Fig. 7E$_2$) and originates posterior to the midline of the element, in contrast to *Janusaurus lundi* where it originates in the middle (Roberts et al. 2014). The dorsal process extends slightly beyond the proximodistal midpoint, which is relatively longer than *Aegirosaurus leptospondylus* (LLD personal observations on SNSB-BSPG 1954 I 608), but shorter than *Arthropterygius chrisorum* (Maxwell 2010) and *Undorosaurus*? *kristiansenae* (Druckenmiller et al. 2012). As in *Keilhauia nui* (Delsett et al. 2017), the deltopectoral crest is restricted to the proximal and anterior portion of the ventral surface. The deltopectoral crest almost reaches the midpoint of the humerus, as in *Janusaurus lundi* (Roberts et al. 2014) and *Arthropterygius chrisorum* (Maxwell 2010), whereas it is longer in *Ophthalmosaurus icenicus* (Moon and Kirton 2016) and *Sisteronia seeleyi* (Fischer et al. 2014a). The humerus has three distal articular facets for the preaxial accessory element, a radius and an ulna, typical of most ophthalmosaurids (Maxwell and Caldwell 2006; Maxwell 2010; Roberts et al. 2014; Fernández and Campos 2015; Paparella et al. 2016; Delsett et al. 2017).

Fig. 7. Postcranial elements of ophthalmosaurid ichthyosaur *Keilhauia* sp. (PMO 222.667) from Spitsbergen, Svalbard, Slottsmøya Member Lagerstätte, → Tithonian. **A**. Interclavicle fused to medial portion of clavicles in ventral (A$_1$, A$_2$) and dorsal (A$_3$) views. Dotted lines represent incomplete margins. **B**. Left clavicle in ventral (B$_1$) and dorsal (B$_2$) views. **C**. Left coracoid in ventral view. **D**. Left scapula in dorsal (D$_1$) and ventral (D$_2$) views. **E**. Right humerus, radius, and ulna in dorsal (E$_1$) and ventral (E$_2$) views. **F**. Atlas-axis in anterior (F$_1$), posterior (F$_2$), and left lateral (F$_3$) views. **G**. Articulated portion of dorsal vertebral column with ribs and neural arches in dorsal view. Photographs (A$_1$, A$_3$, B–G) and interpretative drawings (A$_2$, A$_4$).

In contrast, *Sveltonectes insolitus* (Fischer et al. 2011) and *Nannopterygius enthekiodon* (Hulke 1871) have two facets, whereas *Brachypterygius extremus* (Boulenger 1904) and *Aegirosaurus leptospondylus* (Bardet and Fernández 2000) have a third facet for the intermedium. The ulna and radius facets are separated by a prominent ridge, whereas the facets for the radius and the preaxial accessory element are separated only by a minute ridge. The facet for the preaxial accessory element is circular in proximal view. The ulnar and radial facets are equally anteroposteriorly long, but the facet for the radius is significantly dorsoventrally taller and anteroposteriorly elongated, whereas the facet for the ulna is rectangular. It differs from *Janusaurus lundi* (Roberts et al. 2014) in that the ulnar facet is not as tall relative to the radial facet. The ulnar facet deflects posteriorly, as in *Janusaurus lundi* (Roberts et al. 2014) and *Keilhauia nui* (Delsett et al. 2017), unlike *Gengasaurus nicosiai* where it is not deflected (Paparella et al. 2016).

Epi- and autopodial elements (Fig. 7E): The radius and ulna were complete and found articulated to the humerus. The radius is oval in dorsal view and dorsoventrally taller than the ulna, whereas the ulna is proximodistally longer. The radial facet of the ulna is straight in dorsal view and much taller dorsoventrally than the posterior margin, which is rounded and dorsoventrally very thin. It is not possible to determine the identity of the remaining 20 flattened and more or less circular elements that were found together with the humerus and are interpreted to belong to the same limb. Five elements are approaching the ulna and radius in size and probably represent the preaxial accessory element, proximal and possibly some distal carpals. One element is sickle-shaped, and is probably the pisiform. The 14 smaller elements represent distal carpals and phalanges. One additional forefin element was found close to the skull remains, and it is unknown whether it belongs in the right or left forefin.

Vertebral column and ribs (Fig. 7F, G): The elements in the vertebral column of PMO 222.667 (*Keilhauia* sp.) are well-preserved and complete. The atlas and axis are fully fused to each other (Fig. 7F₃). The axis is almost twice as anteroposteriorly long as the atlas and the suture is well defined in the dorsal half of the element, similar to *Platypterygius australis* (Zammit et al. 2010). The diapophysis fuse with the neural arch facet, whereas the parapophyses are confluent with the anterior edge of the element and are situated in the dorsal half of the centra. In anterior view (Fig. 7F₁), the atlantal surface is rhomboid, whereas the axial surface (Fig. 7F₂) has a more rounded outline as in *Platypterygius australis* (Zammit et al. 2010) and *Arthropterygius chrisorum* (Maxwell 2010). The atlantal surface has the deepest articular surface of the two, as in *Platypterygius americanus* (Maxwell and Kear 2010). The seventeen articulated vertebrae (Fig. 7G) are interpreted as anterior dorsal centra, based on the presence of distinct diapophyses confluent with the neural arch facet (Fischer et al. 2011; McGowan and Motani 2003). The vertebrae are

deeply amphicoelous and pentagonal in anterior view, similar to the anteriormost vertebrae in *Platypterygius americanus* (Maxwell and Kear 2010). The neural canal is flat and bordered by dorsoventrally low, but distinct neural arch facets. The parapophysis and diapophysis are situated on the anterior margin of the vertebrae, which differs from *Arthropterygius chrisorum*, where the parapophyses in the anterior dorsal region are not connected to the anterior edge (Maxwell 2010). In the anteriormost centra, a ridge connects the diapophysis with the parapophysis. Posteriorly, the parapophysis is situated in an increasingly ventral position on the lateral surface, and in the posteriormost preserved vertebrae in the dorsoventral midpoint, similar to *Platypterygius americanus* (Maxwell and Kear 2010). The two facets become deeper and more well-defined posteriorly, as do the neural arch facet. The vertebrae are at least twice as high the length and slightly wider than high, a common relationship for Ophthalmosauridae (Fischer 2012). Their mediolateral width increases rapidly posteriorly in the column, whereas the anteroposterior length only increases slightly. The dorsoventral height has a net increase posteriorly. This is different from *Ophthalmosaurus icenicus* where both width and height increase rapidly in this region (Buchholtz 2001). Two disarticulated vertebrae, found close to the articulated column, are similar in morphology and likely connect to this series. In addition, four disarticulated centra that most likely originate from a more posterior position in the column are preserved. Two of these centra possess smaller apophyses than those in the articulated column, and a third differs from any other by having the two rib facets situated at the same dorsoventral position, one on the anterior and the other on the posterior margin.

Fifteen neural arches were preserved, not fused to the centra. The neural spines are between 20 and 30 mm long and posteriorly inclined. The dorsal end of the neural spines is flat, with small pits indicating a cartilage extension, without the notch found in *Undorosaurus*? *kristiansenae* (Druckenmiller et al. 2012). The prezygapophysis is square or trapezoidal in anterior view and in some neural arches has a dorsoventrally oriented ridge, whereas the postzygapophyses are oval.

The ribs are fractured, and none of them are preserved in their entire length. The most complete rib measures 56 cm. The rib heads are bicipital, with a shorter tuberculum than capitulum. The ribs are unique among ophthalmosaurids in being anteroposteriorly flattened and T-shaped in cross section proximally, with a thickened dorsal margin that is larger on the posterior surface than on the anterior. The midshaft is oval in cross section, whereas the distalmost portion is almost circular. Most ophthalmosaurids have figure eight-shaped ribs at least in the proximal portion (e.g., Maxwell and Kear 2010; Druckenmiller et al. 2012; Moon and Kirton 2016), the exceptions being *Acamptonectes densus* (Fischer et al. 2012) and an Ophthalmosauridae indet. specimen from the SML (PMO 222.670) (Delsett et al. 2017), but both of the latter have instead a rounded cross section.

Remarks.—The proximal articular surface of the humerus is flattened, traditionally used as a criteria for immaturity (Johnson 1977), but many specimens possess this trait regardless of ontogenetic stage (Roberts et al. 2014). The surface of the humerus consists of finished bone, the dorsal and deltopectoral crest are well developed, and the distal articular facets and forefin elements are properly ossified, all indicating an adult stage (Johnson 1977; Kear and Zammit 2014). The fusion of the clavicles to the interclavicle suggest adult (or mature) stage. (Moon and Kirton 2016). Compared to the size of the late juvenile to adult holotype of *Keilhauia* (*Keilhauia nui*, PMO 222.655), the overlapping elements of the new specimen (proximodistal length of humerus and scapula, and anteroposterior length of coracoid) are 40–60% larger (Delsett et al. 2017).

Ophthalmosauridae indet.

Figs. 8, 9.

Material.—PMO 224.252 (Figs. 8, 9, SOM 4: table 2), a partly articulated ichthyosaur that consists of a dorsoventrally compressed and fractured skull with a few postcranial elements. The skull roof, mandibles and a partial palate, consisting of an incomplete parabasisphenoid and pterygoids, are preserved in approximate life position. A large number of teeth are preserved in the anterior portion of the rostrum. The orbital area is not preserved, except for two displaced lacrimals. Both jugals are preserved, but disarticulated and turned 180° so that the anterior ends are directed posteriorly. One hyoid was found disarticulated on the right side of the skull. The quadrates are preserved together in the posterior and left area of the skull, whereas the remainder of the basicranium is missing. The atlas-axis complex is preserved as well as the remains of four smaller vertebrae scattered on top of the skull together with a few ribs and two partial forefin elements. All elements from the specimen share the same preservation: they are severely fractured and some are incomplete, and are dorsoventrally compressed; from Slottsmøya Member Lagerstätte, Tithonian.

Description.—*Premaxilla* (Fig. 8): The rostrum of the Ophthalmosauridae indet. PMO 224.252 is more slender than in *Brachypterygius extremus* (McGowan 1976; SMC J68516, personal observations LLD) and *Undorosaurus? kristianse-nae* (Druckenmiller et al. 2012). The anterior tip of the right premaxilla is situated 70–90 mm posterior to the tip of the dentaries, but because the elements are displaced to some extent it is unknown whether this is due to taphonomic reasons or because the specimen possessed an underbite in life. The premaxilla increases in dorsoventral height posteriorly, as in *Ophthalmosaurus icenicus* and *Palvennia hoybergeti,* in contrast to *Brachypterygius extremus* (McGowan 1976; Druckenmiller et al. 2012; Moon and Kirton 2016), and the element is concave in medial view with a thickened dorsal margin. The anteriormost 15 cm of the lateral surface bears two rows of foramina, one dorsal to the other, that coalesce into one anteroposteriorly directed groove posteriorly. The

groove has a dorsal overhang formed by a sharp ridge and becomes shallower posteriorly. Posteriorly, the dorsal margin of the premaxilla is projected into a minute supranarial process, and the posteroventral margin forms the subnarial process. *Athabascasaurus bitumineus* also has an extremely reduced or absent supranarial process as well as a subnarial posterior process (Druckenmiller and Maxwell 2010). This morphology contrasts the deeply forked posterior end with equal-sized sub- and supranarial processes in *Gengasaurus nicosiai, Caypullisaurus bonapartei,* and *Platypterygius australis* (Kear 2005; Fernández 2007; Paparella et al. 2016). A few cm posterior to the anterior tip in ventral view, starts a series of 12 shallow but clearly demarcated tooth impressions, as in *Ophthalmosaurus icenicus, Platypterygius hercynicus* and *Acamptonectes densus* (Kolb and Sander 2009; Fischer et al. 2012; Moon and Kirton 2016). In *Platypterygius australis* there are 40 shallow impressions (Kear 2005). The tooth impressions do not continue posteriorly as far as the anterior tip of the maxilla, a feature also found in *Pervushovisaurus campylodon, Acamptonectes densus* and *Aegirosaurus leptospondylus* (Bardet and Fernández 2000; Fischer et al. 2012; Fischer 2016), and the alveolar groove is very shallow in this area.

Maxilla (Fig. 8A$_1$, A$_3$): The overall shape of the maxilla in the Ophthalmosauridae indet. specimen PMO 224.252 resembles *Ophthalmosaurus icenicus* (Moon and Kirton 2016). The lateral surface is convex, with a triangular and mediolaterally thin dorsal flange and a thickened ventral portion. The maximum dorsoventral height of the element is encountered approximately midway anteroposteriorly, and approaches that of the premaxilla, in contrast to *Sveltonectes insolitus* where the maxilla is very reduced compared to other elements in this region (Fischer et al. 2011). The dorsal margin and the lateral surface in the anterior portion of the element is smoother than the more posterior portion, which has a crenulated margin and a lateral surface with longitudinal ridges, probably for contact with the lacrimal and/or the jugal (Druckenmiller et al. 2012; Fischer et al. 2014b; Moon and Kirton 2016). The dorsal margin is not made up of a series of processes as in *Platypterygius australis* (Kear 2005). The posterior portion of the element is drawn out into a long, narrow process, as in many ophthalmosaurids, e.g. *Palvennia hoybergeti* and *Brachypterygius extremus* (Druckenmiller et al. 2012; McGowan 1976). The alveolar groove does not show tooth impressions.

Jugal (Fig. 8): The suborbital bar of the jugal in Ophthalmosauridae indet. PMO 224.252 tapers anteriorly and is mediolaterally thicker than the posteriorly ascending process. The posteroventral corner is dorsoventrally and anteroposteriorly wider and more similar to *Janusaurus lundi* (Roberts et al. 2014) and *Leninia stellans* (Fischer et al. 2013b) than to the narrow corner of *Palvennia hoybergeti* (Delsett et al. 2018). The amount of curvature from the suborbital bar to the posteriorly ascending process is similar to *Palvennia hoybergeti* and *Ophthalmosaurus icenicus*, contrasting the straighter
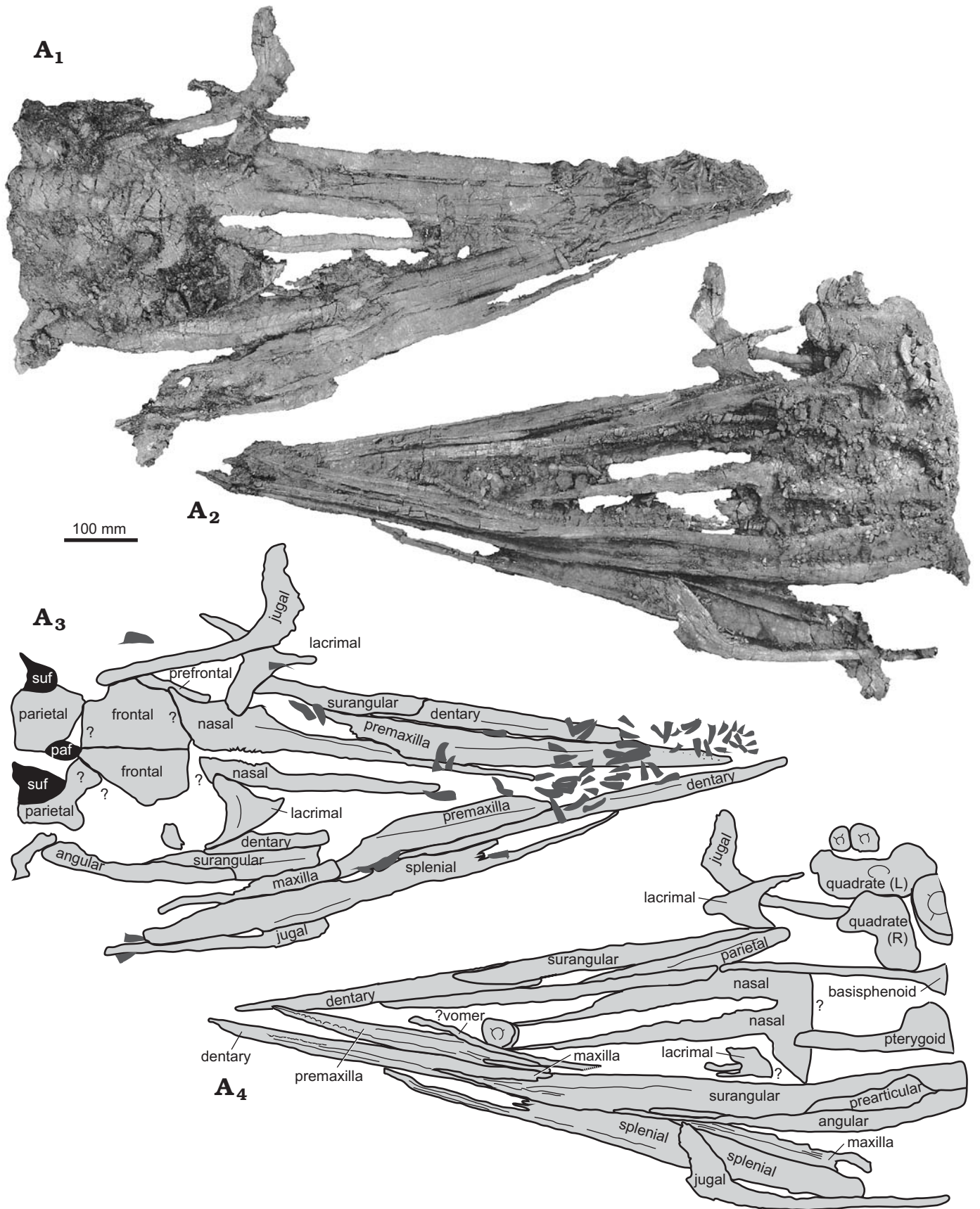
Fig. 8. Skull of Ophthalmosauridae indet. (PMO 224.252) from Spitsbergen, Svalbard, Slottsmøya Member Lagerstätte, Tithonian; in dorsal (A_1, A_3) and ventral (A_2, A_4) views. Photographs (A_1, A_2) and interpretative drawings (A_3, A_4). L, left; R, right; paf, parietal foramen; suf, supratemporal fenestra.

jugal in *Undorosaurus*? *kristiansenae* (Druckenmiller et al. 2012, Moon and Kirton 2016). The posteriorly ascending process is relatively anteroposteriorly wide, similar to some *Ophthalmosaurus icenicus* specimens (e.g., CAMSM J29861; personal observations LLD) and *Palvennia hoybergeti* (Delsett et al. 2018). The posterior outline of the posterior process is crenulated.

Nasal (Fig. 8): The anterior process of the nasal is thin and increases steadily in mediolateral width posteriorly. Except for the thin anteriormost portion, the nasal has the typical 90° bend forming a lateral extension found in most ophthalmosaurids (Kear 2005; Fischer et al. 2012; Moon and Kirton 2016; Delsett et al. 2018). As preserved there is a 30 mm wide gap between the anterior portions of the nasals, which abruptly decreases in width posteriorly. The gap is probably taphonomic, as the nasals meet in a medial butt joint in *Ophthalmosaurus icenicus* (Moon and Kirton 2016), but it might partly represent a vacuity or an internasal foramen, a structure that is found in some ophthalmosaurids, e.g., *Sveltonectes insolitus*, however usually more posteriorly (Fischer et al. 2011). In the posterior portion the element flares out into a lateral wing as in other ophthalmosaurids (Kear 2005; Fischer et al. 2012). On the left side the lateral wing covers the prefrontal posterior to the narialis process. The medial margin of the nasal in this area is crenulated as in *Platypterygius australis* (Kear 2005). The posterior margins of the nasals are incompletely preserved, but clearly overlap the frontals on the left side of the skull where the preservation is best, and there is a lack of contact between the nasals and the parietals, similar to other ophthalmosaurids e.g., *Platypterygius australis* (Kear 2005).

Frontal (Fig. 8A$_1$, A$_3$): The frontals are preserved in articulation in PMO 224.252 (Ophthalmosauridae indet.). They are overlapped by the nasals anteriorly and overlap the parietals posteriorly, but with incompletely preserved margins. There is a lack of interdigitating structures between the skull roof elements, in contrast to *Acamptonectes densus* (Fischer et al. 2012). The exact relationship with the parietal foramen is unknown, but the frontals meet its anterior border and possibly surround it laterally. In contrast to platypterygiine ophthalmosaurids, the frontals seem not to have extended to the anterior margin of the supratemporal fenestra (Kear 2005; Fischer et al. 2014b). The two frontals meet in a straight suture as in *Ophthalmosaurus icenicus* (Moon and Kirton 2016) in contrast to the crenulated and interlocking margin in *Platypterygius australis* and *Athabascasaurus bitumineus* (Kear 2005; Druckenmiller and Maxwell 2010). The element is flat, in contrast to the deeply concave frontal in *Platypterygius australis* (Kear 2005), and it possesses a processus temporalis, which is thin and stretches laterally under the jugal on the left side.

Parietal (Fig. 8A$_1$, A$_3$): The parietals are not complete posteriorly, and the right parietal preserves incomplete sutures to other elements. The dorsal surface of the parietal is slightly convex as in *Palvennia hoybergeti* (Druckenmiller et al. 2012), and not concave as in *Gengasaurus nicosiai*

(Paparella et al. 2016). As preserved, the parietals border most of the parietal foramen laterally and posteriorly, but might have been overlain by the frontals in the anterior portion. In contrast, the parietals of *Platypterygius hercynicus* are excluded from contact with the parietal foramen (Fischer 2012). The parietals do not contact the prefrontal. The parietal foramen is anteroposteriorly elongated, and of the same relative size as in other ophthalmosaurids (Maxwell et al. 2015; Moon and Kirton 2016) and not enlarged as is autapomorphic for *Palvennia hoybergeti* (Druckenmiller et al. 2012; Delsett et al. 2018). The supratemporal fenestra is not reduced and its anterior margin reaches halfway into anteroposterior length of the parietal foramen.

Lacrimal (Fig. 8): The left lacrimal is preserved in medial view and the right in lateral view in Ophthalmosauridae indet. PMO 224.252. The element has an anterior, a posterodorsal and a ventral process and is similar in overall shape to *Palvennia hoybergeti* (Druckenmiller et al. 2012). The anterior process is dorsoventrally taller than the posterior and drawn out into a small, triangular process that is similar to in shape but dorsoventrally taller than in *Palvennia hoybergeti* (Druckenmiller et al. 2012) and *Janusaurus lundi* (Roberts et al. 2014). The dorsal process is of the same width as the anterior process. The anterior process is mediolaterally thin anteriorly and thicker along the posterior margin, where it has a ridge on the medial surface. The posterior process is a single narrow process, not a number of finger-like projections as in *Platypterygius australis* (Kear 2005). Similar to *Leninia stellans* (Fischer et al. 2013b) the posterior process is anteroposteriorly long compared to the middle portion, compared to *Undorosaurus*? *kristiansenae* where the posterior process is relatively shorter (Druckenmiller et al. 2012). The middle portion of the element is relatively large as in *Caypullisaurus bonapartei* (Fernández 2007) and *Platypterygius americanus* (McGowan 1972), but smaller than in *Simbirskiasaurus birjukovi* (Fischer et al. 2014b). The lateral surface bears a diagonal ridge for the anteroposterior margin of the orbit, as in *Athabascasaurus bitumineus* and *Sveltonectes insolitus* (Druckenmiller and Maxwell 2010; Fischer et al. 2012). On the medial surface are two slight depressions and a small ridge, probably for articulation with the maxilla (Moon and Kirton 2016). The posterior margin is curved although not to the near to 90° autapomorphic bend of *Undorosaurus*? *kristiansenae* (Druckenmiller et al. 2012). The ventral surface of the middle portion is grooved.

Pterygoid (Fig. 8A$_2$, A$_4$): Two partial pterygoids are preserved in the Ophthalmosauridae indet. specimen PMO 224.252. The posterior portion is missing in both elements, and the medial sheet and anterior processes do not preserve details. As in other ophthalmosaurids, the medial sheet is dorsoventrally flattened and mediolaterally wider than the more anterior portion that is instead dorsoventrally thicker.

Parabasisphenoid (Fig. 8A$_2$, A$_4$): The only preserved part of the parabasisphenoid in PMO 224.252 is the majority of the anterior parasphenoid process (cultriform process). The preserved process is equally mediolaterally wide for
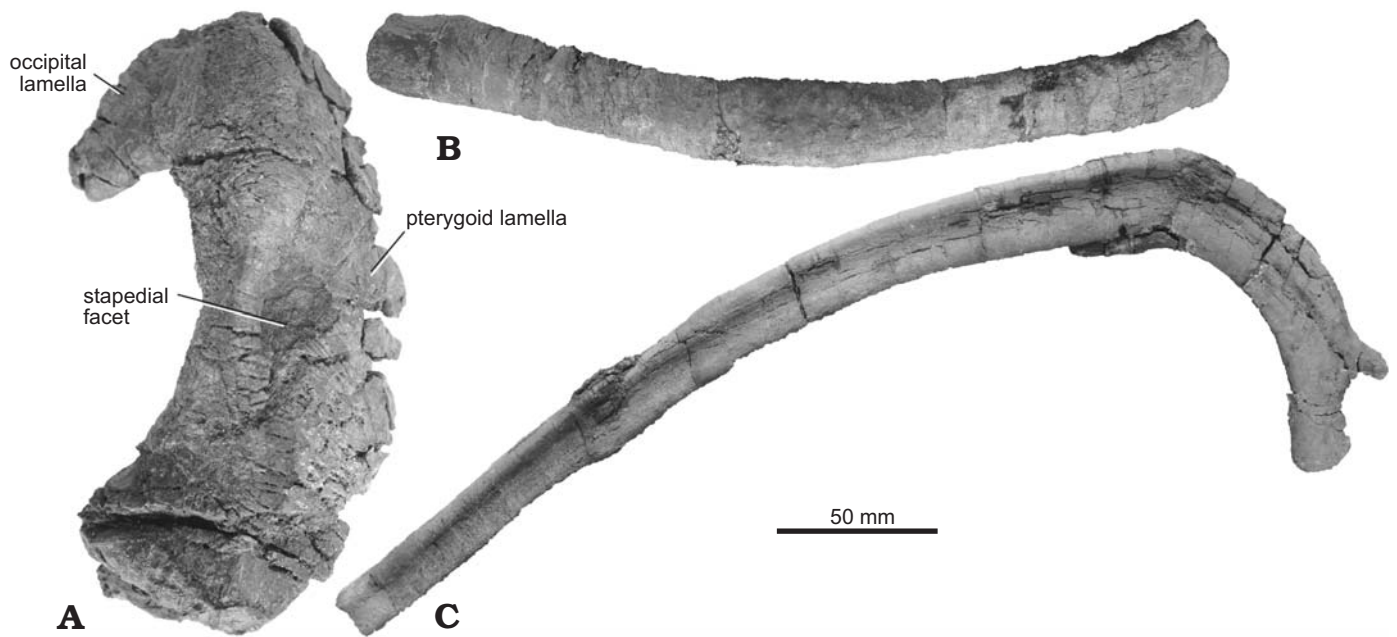
Fig. 9. Elements of Ophthalmosauridae indet. (PMO 224.252) from Spitsbergen, Svalbard, Slottsmøya Member Lagerstätte, Tithonian. **A**. Left quadrate in posterior view. **B**. Hyoid in anterior or posterior view. **C**. Rib in anterior or posterior view.

its entire length, and widens mediolaterally for articulation with the basisphenoid posteriorly.

Quadrate (Figs. 8A$_2$, A$_4$, 9A): Both quadrates are preserved in Ophthalmosauridae indet. PMO 224.252, and the description is based on the better preserved left element which is nearly complete, with only an incomplete medial margin (Fig. 9A). The dorsal portion of the occipital lamella is triangular in posterior view and has a lateral reach approximately similar to that of the articular condyle. It is of approximately the same relative size as *Ophthalmosaurus icenicus* and *Palvennia hoybergeti* (Moon and Kirton 2016; Delsett et al. 2018), while *Platypterygius australis* and *P. hercynicus* lack the lateral extension of the occipital lamella (Kear 2005; Kolb and Sander 2009). The quadrate foramen ventral to the occipital lamella is relatively smaller than in *Ophthalmosaurus icenicus* (Moon and Kirton 2016). The pterygoid lamella covers a smaller area than in *Ophthalmosaurus icenicus* and *Palvennia hoybergeti* and is dorsoventrally straight in posterior view compared to the rounded outline in these taxa (Moon and Kirton 2016; Delsett et al. 2018). Quadrate outline is however variable in *Ophthalmosaurus icenicus* (Moon and Kirton 2016; e.g., rounded in GLAHM V1852 and straighter in MANCH L10304 personal observations AJR and LEIUG 90986 personal observations LLD). The pterygoid lamella is dorsoventrally taller relative to mediolateral width than in *Sisteronia seeleyi* (Fischer et al. 2014a). A ridge separates the occipital and pterygoid lamellae as in the Ophthalmosaurinae indet. specimen UAMES 3411 (Druckenmiller and Maxwell 2013) but in contrast to PMO 222.667 which has no such ridge. The ridge is formed by a convex surface in the dorsal portion of the quadrate and a distinct dorsoventrally oriented ridge ventral to the stapedial facet as in *Palvennia hoybergeti* (Delsett et al. 2018).

The stapedial facet on the posterior surface is large and as in *Palvennia hoybergeti* it is situated in a more dorsal position than in *Ophthalmosaurus icenicus* and *Platypterygius australis* (Kear 2005; Moon and Kirton 2016; Delsett et al. 2018). The facet is dorsoventrally elongated with a thickened lateral and ventral margin as in *Sisteronia seeleyi* and *Sveltonectes insolitus* (Fischer et al. 2011; Fischer et al. 2014a). The articular condyle is relatively small compared to the rest of the element, compared to *Acamptonectes densus* and "*Grendelius*" *alekseevi* (Fischer et al. 2012; Zverkov et al. 2015a). In ventral view, the articular condyle bears the surangular and articular facets on each side of a depression in ventral view. The anterior surface of the element is concave and featureless.

Dentary (Fig. 8): The anterior tip of the dentary is straight as in *Acamptonectes densus* (Fischer et al. 2012). The dorsal and ventral margins curve around the dorsal and ventral margins of the surangular. The dentary is dorsoventrally narrow compared to anteroposterior length and resembles *Aegirosaurus leptospondylus* (Bardet and Fernández 2000; LLD personal observations on SNSS-BSPG 1954 I 608) more than the more robust dentaries in *Palvennia hoybergeti*, *Undorosaurus*? *kristiansenae* (Druckenmiller et al. 2012) and *Brachypterygius extremus* (McGowan 1976). In the anterior portion of the lateral surface are two rows of anteroposteriorly elongated foramina, as in *Acamptonectes densus* (Fischer et al. 2012) and the *Palvennia hoybergeti* specimen PMO 222.669 (Delsett et al. 2018). Posteriorly the foramina coalesce into a deep longitudinal groove that becomes shallower posteriorly as in *Sveltonectes insolitus* and *Platypterygius australis* (Kear 2005; Fischer et al. 2011). The alveolar groove is shallower than in *Palvennia hoybergeti* (Delsett et al. 2018), and the anterior portion is parti-

tioned into shallow tooth impressions as in *Platypterygius australis* (Kear 2005). On the medial surface the ventral margin is thickened, which forms a groove to the ventral margin that represents the anterior portion of the Meckelian canal (Moon and Kirton 2016; Kear 2005). The element has a diagonal posterior margin.

Splenial (Fig. 8): The total length of the splenial is less than the surangular, and it is slightly dorsoventrally shorter anteriorly than posteriorly as in *Acamptonectes densus* (Fischer et al. 2012). As in *Palvennia hoybergeti* and *Ophthalmosaurus icenicus* (Moon and Kirton 2016; Delsett et al. 2018), the anterior, bifurcated portion, ("anterior fork") is strongly elongated in contrast to *Platypterygius australis* (Kear 2005). In contrast to all of these, the anterior fork in PMO 224.252 has two additional, smaller processes between the dorsal and ventral processes. The opening between the two small processes might correspond to the tiny foramen found in *Baptanodon natans* (Gilmore 1906). As in *Palvennia hoybergeti* (Delsett et al. 2018) one of the long processes is concave. Posterior to the fork, the element has a thickened dorsal ridge on the lateral surface, decreasing in size posteriorly, as in *Ophthalmosaurus icenicus* (Moon and Kirton 2016). The element lacks the ventral semicircular ridge which is found in *Pervushoisaurus bannovkensis* (Fischer et al. 2014b).

Angular (Fig. 8A$_2$, A$_4$): The right angular is preserved in articulation with the surangular and the prearticular, and lacks the posteriormost portion. The element is medially and laterally slightly convex, in contrast to *Sveltonectes insolitus*, which is medially and laterally concave (Fischer et al. 2011). It has an extensive lateral exposure, common to all ophthalmosaurids (Bardet and Fernández 2000; Fernández and Campos 2015; Fischer et al. 2012). In contrast to *Palvennia hoybergeti,* the element has a long and narrow anterior process (Delsett et al. 2018) as found in other ophthalmosaurids (e.g., Druckenmiller et al. 2012; Moon and Kirton 2016). It does, however, extend shorter anteriorly than the surangular, in contrast to *Aegirosaurus leptospondylus* and *Platypterygius australis* where the two elements are of the same length (Bardet and Fernández 2000; Kear 2005). The element increases in dorsoventral height posteriorly as in *Ophthalmosaurus icenicus* (Moon and Kirton 2016) and is dorsoventrally tallest anterior to the dorsoventral maximum height of the prearticular, where it contributes less than half to the total height of the ramus in medial view.

Prearticular (Fig. 8A$_2$, A$_4$): The right prearticular is preserved in articulation between the surangular and angular in medial view, and lacks the posterior bar. The angular reaches further anteriorly than the prearticular in medial view, as in *Janusaurus lundi* (Roberts et al. 2014). The dorsal margin is gently curved in lateral view as in *Ophthalmosaurus icenicus*, *Janusaurus lundi* and *Palvennia hoybergeti* (Roberts et al. 2014; Moon and Kirton 2016; Delsett et al. 2018) in contrast to the pointed margin in *Platypterygius australis* (Kear 2005). The dorsoventral maximum height is approximately one centimeter shorter than the height of the surangular.

Surangular (Fig. 8): The description is mainly based on the right surangular, which is preserved articulated to the prearticular, angular and dentary. The anterior tip is dorsoventrally short and increases in height posteriorly as in other ophthalmosaurids (e.g., Druckenmiller et al. 2012; Moon and Kirton 2016). The dorsal and ventral margins are thickened and rounded, and due to this, the anterior portion of the medial surface is more concave than in *Palvennia hoybergeti* (Delsett et al. 2018) but resembles *Platypterygius hercynicus* and *P. australis* in this aspect (Kear 2005; Kolb and Sander 2009). In lateral view, the surangular possesses a fossa surangularis, as in e.g. *Pervushovisaurus bannovkensis*, in contrast to *Sveltonectes insolitus,* which lacks this feature (Fischer et al. 2011, 2014b). The element is dorsoventrally tallest in the posterior portion, corresponding to the maximum dorsoventral height of the prearticular. The posteriormost portion is not preserved.

Dentition (Fig. 8A$_1$, A$_3$): Approximately 140 teeth are preserved in PMO 224.252 (Ophthalmosauridae indet.), not in life position, but what is likely an almost correct order, i.e. the smallest teeth are preserved at the anteriormost portion of the rostrum. The teeth are poorly preserved, and few details from the surface can be described. Compared to other ophthalmosaurids, they are of an intermediate size and robustness: smaller than in *Brachypterygius extremus* and larger than in *Aegirosaurus leptospondylus*, and more similar to e.g., *Palvennia hoybergeti* (McGowan 1976; Bardet and Fernández 2000; Delsett et al. 2018; LLD personal observations on SMC J68516 and SNSS-BSPG 1954 I 608). There is a significant increase in height and diameter of the teeth moving posteriorly in the jaw, from a total height of 16 mm in the anteriormost teeth to 41 mm in the largest, more posterior teeth, which is a wider size range than in *Palvennia hoybergeti* (Delsett et al. 2018). The crown and root are subtly ridged, with ridges that are more uneven in the root. The roots have an approximate rectangular cross section, with the shorter sides in the rectangle perpendicular to the curvature direction of the teeth. The corners of the rectangle are not well-defined.

Hyoid (Fig. 9B): The hyoid of Ophthalmosauridae indet. PMO 224.252 was found disarticulated on the right side of the skull, and is tentatively interpreted as the right. The element is almost straight as in *Janusaurus lundi* and *Sveltonectes insolitus* (Fischer et al. 2011; Roberts et al. 2014) and differs from the more curved hyoids in *Platypterygius hercynicus* (Kolb and Sander 2009) and PMO 222.667. The anterior end is mediolaterally thicker than the posterior end, as in *Janusaurus lundi* (Roberts et al. 2014) and has an oval cross section. The anterior end is, in contrast, flattened in *Gengasaurus nicosiai* (Paparella et al. 2016) and *Sveltonectes insolitus* (Fischer et al. 2011). The lateral surface (facing the mandible) of the hyoid in PMO 224.252 is flattened and bears a shallow groove, while the medial surface is convex.

Vertebral column and ribs: The five preserved vertebrae of Ophthalmosauridae indet. PMO 224.252 vary largely in size. The atlas-axis is the largest, and has one pentagonal

surface whereas the other is too poorly preserved for description. On the lateral surface is a single rib facet in the dorsal half on each side, but there was very likely a more ventrally placed facet as the short, presumably "cervical" rib is bicipital. One vertebra is interpreted as dorsal because its two lateral rib facets are confluent with the anterior margin (McGowan and Motani 2003). The smallest vertebral remains are interpreted to belong to caudal centra.

The neural arch of either the atlas or the axis is anteroposteriorly narrow, but too poorly preserved to warrant a description.

The rib fragments vary in size. The shortest, which is the only complete rib, is 11 cm, and is interpreted to be from the anteriormost portion ("cervical") of the vertebral column. The longest rib was at least four times as long (Fig. 9C). The proximal heads of the ribs, where preserved, are bicapitate and they have a thickened dorsal margin, resulting in a T-shaped cross section in contrast to the typical figure eight cross section in ophthalmosaurids, but similar to PMO 222.667 in this aspect. The distalmost portion of the rib is subcircular in cross section and longitudinally striated which is uncommon among ophthalmosaurids, but found in the Ophthalmosauridae indet. specimen PMO 222.670 (Delsett et al. 2017) and *Palvennia hoybergeti* (Delsett et al. 2018).

Remains from some gastralia are present, but none of them are complete. As in *Ophthalmosaurus icenicus, Janusaurus lundi, Palvennia hoybergeti* and *Keilhauia nui* they are circular to subcircular in cross section (Roberts et al. 2014; Moon and Kirton 2016; Delsett et al. 2017, 2018).

Forefin elements: One complete but deformed, and one partial forefin element are preserved of the Ophthalmosauridae indet. specimen PMO 224.252. The complete element is oval in dorsal and ventral view and strongly thickened, and based on comparison to *Palvennia hoybergeti* (Delsett et al. 2018), it might be a metacarpal. The less complete element is relatively small and circular in dorsal and ventral view, and is most likely a phalanx.

Remarks.—The preserved skull lacks the posteriormost portion of the lower mandibles and the basicranium, but by comparison to the holotype of *Undorosaurus*? *kristiansenae* and *Ophthalmosaurus icenicus* (Druckenmiller et al. 2012; Moon and Kirton 2016), it is estimated that the preserved remains represent approximately 85% of total skull length. This gives an estimated total skull length in life of 1280 mm, which is longer than the holotypes of *Palvennia hoybergeti* (SVB 1451) and *Undorosaurus*? *kristiansenae* (PMO 214.578), the latter with a total body length of 5.5 meters (Druckenmiller et al. 2012). The surface of the ribs and the best preserved skull elements display finished bone. Even though the typical ontogenetic criteria cannot be assessed (Johnson 1977, Kear 2005), the large size and surface texture where accessible are valid indicators of an adult stage.

Genus *Undorosaurus* Efimov, 1999

Type species: *Undorosaurus gorodischensis* Efimov, 1999; Volga region near Unlyanovsk, Gorodischi, Middle Volgian.

Undorosaurus? *kristiansenae* Druckenmiller, Hurum, Knutsen, and Nakrem, 2012

Fig. 10.

Holotype: PMO 214.578, complete skeleton primarily described by Druckenmiller et al. (2012); basioccipital, basisphenoid, and stapes are described herein for the first time.

Material.—Type material only (Fig. 10, SOM 4: table 3).

Emended diagnosis.—Large ophthalmosaurid ichthyosaur (estimated 5.5 m total body length) with the following autapomorphies and unique character combinations: robust rostrum with snout ratio of 0.61 (relatively longer and more gracile in *Aegirosaurus, Nannopterygius*); orbital ratio of 0.19 (relatively larger in *Ophthalmosaurus, Nannopterygius*); supranarial process of premaxilla strongly reduced and not contacting the external naris (well-developed supranarial process contacting the external naris in *Brachypterygius* and *Caypullisaurus*); subnarial process does not contact the jugal (contacts jugal in *Brachypterygius*); lacrimal does not contact the external naris (contacts external naris in *Ophthalmosaurus, Caypullisaurus, Aegirosaurus, Sveltonectes*); posterior margin of lacrimal forms distinct, nearly 90° angle (autapomorphic); maxilla with 23 teeth (10–13 in *Ophthalmosaurus*); maxilla with extensive lateral exposure along the tooth row, extending as far posteriorly as the midpoint of the orbit (shorter exposure laterally in *Brachypterygius, Aegirosaurus, Ophthalmosaurus*); jugal nearly straight (bowed in *Aegirosaurus, Ophthalmosaurus*); postorbital bar anteroposteriorly broad (narrow in *Ophthalmosaurus, Aegirosaurus, Nannopterygius*); element (supratemporal?) located posterior to the quadratojugal with a narrow, ventrally projecting process (autapomorphic); large exposure of extracondylar area in posterior view (little or no exposure in *Palvennia, Janusaurus, Simbirskiasauru*s, *Arthropterygius, Sisteronia*, and *Platypterygius australis*); large basipterygoid processes on basisphenoid (small or non-existent in *Palvennia hoybergeti, Arthropterygius chrisorum, Sisteronia seeleyi*); teeth robust and large with numerous, fine, enamelled ridges (relatively smaller and more gracile in *Aegirosaurus* and *Sveltonectes*); 52 presacral vertebrae (39–42 in *Ophthalmosaurus*, 37? in *Platypterygius americanus*); conspicuous V-shaped notch along the dorsal margin of presacral neural spines as seen in lateral view (autapomorphic among ophthalmosaurids); ribs 8-shaped in cross section (round in *Acamptonectes*); relatively small forelimb bearing 5–6 digits (relatively larger with 6+ digits in *Caypullisaurus, Platypterygius*); humerus with two distal facets only (three facets in *Ophthalmosaurus, Aegirosaurus, Caypullisaurus, Undorosaurus, Brachypterygius, Arthropterygius, Acamptonectes, Palvennia*); rounded phalanges (rectangular in *Platypterygius, Sveltonectes*); ischiopubis expanded and unfused distally (unlike *Ophthalmosauru*s, *Keilhauia, Platypterygius australis, Sveltonectes, Aegirosaurus, Caypullisaurus*); femur anteroposteriorly broad with two facets distally (three distal facets in *Platypterygius americanus, P. australi*s).
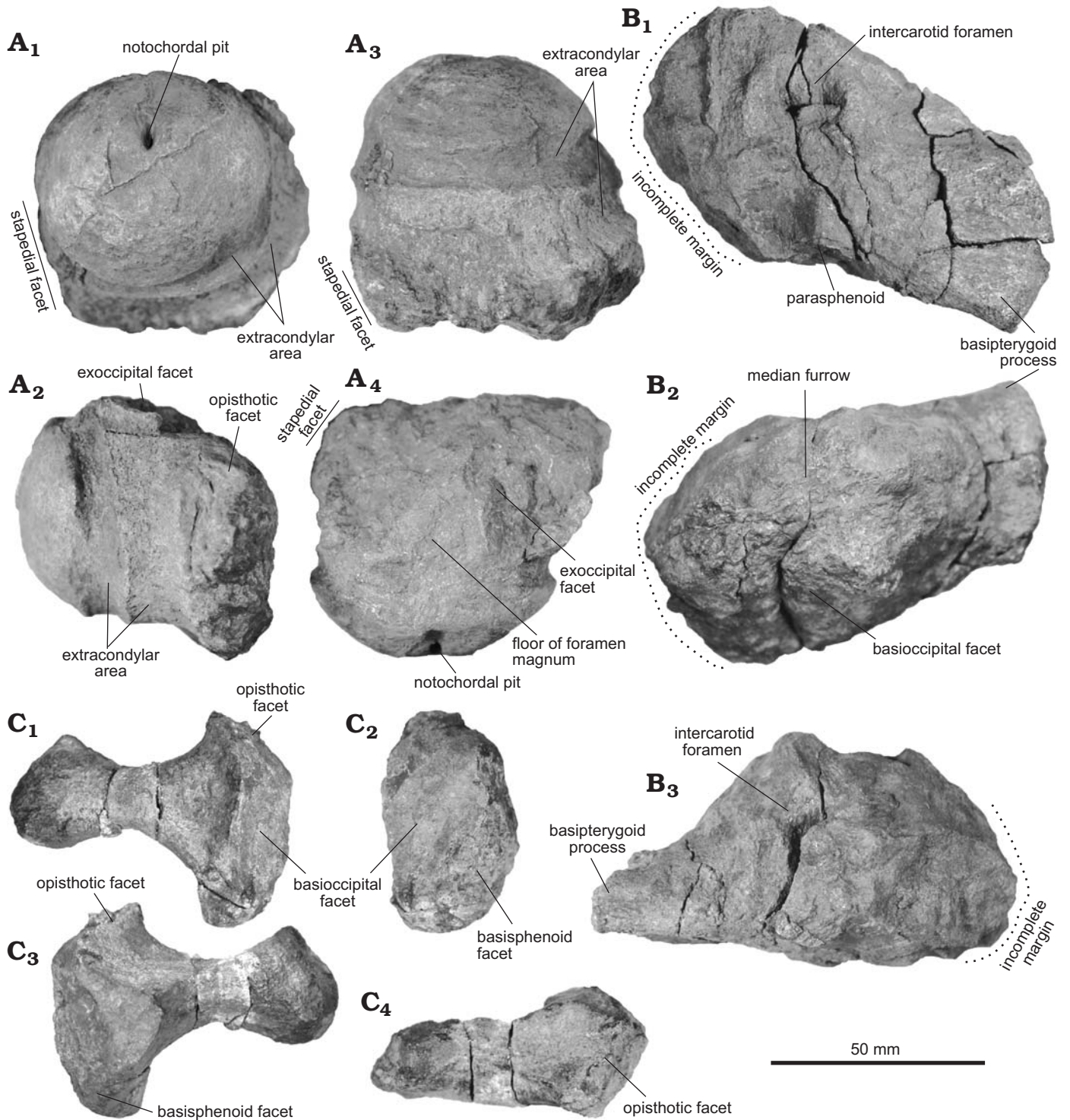
Fig. 10. Basicranium of ophthalmosaurid ichthyosaur *Undorosaurus? kristiansenae* Druckenmiller, Hurum, Knutsen, and Nakrem, 2012 (PMO 214.578, holotype) from Spitsbergen, Svalbard, Slottsmøya Member Lagerstätte, Tithonian. **A**. Basioccipital posterior (A_1), right lateral (A_2), ventral (A_3) and dorsal (A_4) views. **B**. Basisphenoid in ventral (B_1), dorsal (B_2), and anterior (B_3) views. **C**. Left stapes in posterior (C_1), medial (C_2), anterior (C_3), and dorsal (C_4) views.

Description.—Basioccipital (Fig. 10A): The dorsal and parts of the left lateral surfaces of the basioccipital from PMO 214.578 (*Undorosaurus? kristiansenae*) are damaged. The floor of the foramen magnum is narrowest anteriorly and increases in mediolateral width posteriorly (Fig. 10A$_4$). In posterior view (Fig. 10A$_1$), the occipital condyle is slightly medio-

laterally wider than dorsoventrally tall and the extracondylar area is largely visible. Surrounding the condyle on all sides is a ring of unfinished bone. Anterior to this is a wider extracondylar area forming a second ring on the lateral and ventral surfaces, also visible in posterior view (Fig. 10A$_2$). This is different from PMO 222.667, *Simbirskiasaurus bir-*

jukovi (Fischer et al. 2014b), *Arthropterygius chrisorum* (Maxwell 2010), *Sisteronia seeleyi* (Fischer et al. 2014a), *Palvennia hoybergeti* (Delsett et al. 2018) and *Platypterygius australis* (Kear 2005), which have little or no extracondylar area visible in posterior view. The morphology resembles *Ophthalmosaurus icenicus*, *Athabascasaurus bitumineus* and *Acamptonectes densus* (Druckenmiller and Maxwell 2010; Fischer et al. 2012; Moon and Kirton 2016), but this specimen has even more extensive extracondylar area exposed in posterior view and the condyle is more clearly set off from the extracondylar area. The basioccipital is not preserved in the holotype of *Undorosaurus gorodischensis*, but in another specimen attributed to the species, the basioccipital displays a similar overall shape (Zverkov and Efimov 2019). The extracondylar area visible in posterior view in *Undorosaurus gorodischensis* (Zverkov and Efimov 2019: fig. 6B, D) is relatively wide for an ophthalmosaurid, but not as extreme as that found in PMO 214.578. The notochordal pit in PMO 214.578 consists of only one pit, in contrast to PMO 222.667 (*Keilhauia* sp.) and *Undorosaurus gorodischensis* (Zverkov and Efimov 2019: fig. 6A) and the *Undorosaurus* sp. specimen UPM-EP-II-23(744). The notochordal pit is situated more dorsally than in *Arthropterygius chrisorum* (Maxwell 2010) and *Janusaurus lundi* (Roberts et al. 2014) but more ventrally than in *Brachypterygius extremus* (McGowan 1976). In lateral view, the stapedial and opisthotic facets are poorly separated from each other. Anteriorly on the ventral surface is a depression, probably representing a shallow ventral notch. The anteriormost portion of the element is significantly larger and more drawn out ventrally in PMO 214.578 than in *Undorosaurus gorodischensis* (UPM EP-II-21(1075) (Zverkov and Efimov 2019). *Palvennia hoybergeti* and *Acamptonectes densus* lack a ventral notch, whereas this structure is found in *Ophthalmosaurus icenicus* (Fischer et al. 2012; Moon and Kirton 2016; Delsett et al. 2018). Because of preservation it is unknown whether the specimen possessed a basioccipital peg.

Basisphenoid (Fig. 10B): The basisphenoid from PMO 214.578 (*Undorosaurus? kristiansenae*) is damaged on the left side and has suffered deformation along the sagittal plane. The element is anteroposteriorly short compared to mediolateral width and dorsoventrally tall relative to anteroposterior length, compared to almost all other ophthalmosaurids, except *Undorosaurus gorodischensis* and *Sveltonectes insolitus* which are also relatively dorsoventrally tall (Fischer et al. 2011; Zverkov and Efimov 2019). This might be affected to some degree by the deformation. The dorsal plateau covers a relatively small area and is coarsely rugose with a wide median furrow. The anterior, posterior and lateral surfaces slope steeply from the dorsal surface. The anterior carotid foramen is situated in the mediolateral and dorsoventral midpoint of the anterior surface and is smaller than the ventral foramen. Almost the entire posterior surface is taken up by the basioccipital facet. The ventral surface (Fig. 10B$_1$) is flat with the base of the parasphenoid anterior to the carotid foramen,

as in *Ophthalmosaurus icenicus*, *Mollesaurus periallus*, and *Platypterygius australis* (Fernández 1999; Kear 2005; Maxwell 2010; Moon and Kirton 2016). The parasphenoid has an oval cross section in anterior view and the same mediolateral width as the foramen. The carotid foramen is bordered by ridges laterally and anteriorly as in *Sisteronia seeleyi* (Fischer et al. 2014a). A ventral carotid foramen is found in *Undorosaurus gorodischensis*, *Ophthalmosaurus icenicus*, and *Brachypterygius extremus* (McGowan 1976, Moon and Kirton 2016, Zverkov and Efimov 2019) in contrast to the posterior foramen in *Arthropterygius chrisorum* (Maxwell 2010), *Palvennia hoybergeti* (Delsett et al. 2018) and PMO 222.667. In ventral view the basipterygoid process is among the largest in any ophthalmosaurid (Fischer et al. 2014a, Kirton 1983, Maxwell 2010), even larger than in *Platypterygius australis* (Kear 2005), *Mollesaurus periallus* (Fernández 1999; AJR personal observation on MOZ 2282 V), *Brachypterygius extremus* (McGowan 1976) and *Undorosaurus gorodischensis* (Zverkov and Efimov 2019).

Stapes (Fig. 10C): The two stapes from PMO 214.578 (*Undorosaurus? kristiansenae*) were oriented based on the articulation of the left to the basioccipital and their similarity to *Palvennia hoybergeti* (Delsett et al. 2018) with a flatter posterior surface. The left stapes (Fig. 10C) is better preserved than the right, which is compressed and distorted. The overall morphology, especially relative size of the medial and lateral heads and shaft outline is most similar to *Platypterygius australis* (Kear 2005) in constrast to the more slender stapes in *Janusaurus lundi* (Roberts et al. 2014). The medial head is dorsoventrally taller than anteroposteriorly long in medial view. The facet for the opisthotic is small and poorly demarcated. The facet for the basioccipital is the largest as in the Ophthalmosaurinae indet. specimen UAMES 3411 (Druckenmiller and Maxwell 2013) and faces posteromedially with an anterior margin that is well defined by a dorsoventrally oriented ridge. Ventral to the basioccipital facet is the less well-defined basisphenoid facet. The shaft of the stapes has approximately the same relative thickness as in *Platypterygius australis* (Kear 2005) and *Ophthalmosaurus icenicus* (Moon and Kirton 2016), which is anteroposteriorly and dorsoventrally thicker than in *Janusaurus lundi* (Roberts et al. 2014) and *Palvennia hoybergeti* (Druckenmiller et al. 2012), but more gracile than in *Sisteronia seeleyi* (Fischer et al. 2014a) and *Leninia stellans* (Fischer et al. 2013b). The shaft is pyriform in cross section, in contrast to the rounded cross section in the shaft of *Janusaurus lundi* (Roberts et al. 2014) as in *Platypterygius australis* (Kear 2005). The lateral head is expanded both dorsally and ventrally as in *Platypterygius australis* (Kear 2005), in contrast to *Acamptonectes densus* (Fischer et al. 2012), *Janusaurus lundi* (Roberts et al. 2014) and *Palvennia hoybergeti* (Druckenmiller et al. 2012), which have small lateral heads barely expanded relative to the shaft. The lateral head bears a triangular facet for the quadrate on its lateral surface. With regard to *Undorosaurus gorodischensis*, overlapping braincase material of the two holotype specimens PMO 214.578 and UPM EP-II-20(572) is only based on the sta-

pes. It is not as slender and constricted in UPM EP-II-20(572) (Zverkov and Efimov 2019: fig. 5E, F) as in PMO 214.578. In medial view UPM EP-II-20(572) is teardrop shaped (Zverkov and Efimov 2019: fig. 5I), while PMO 214.578 is oval. The fragmentary stapes in UPM EP-II-23(744) cannot be interpreted (Zverkov and Efimov 2019: fig. 6H, I).

Remarks.—Most of the reinterpretations by Zverkov and Efimov (2019) seem to be correct, but some misinterpretations are summarized here, as it is of value to the hypothesized synonymy of *Undorosaurus gorodischensis* and *Cryopterygius kristiansenae* (Zverkov and Efimov 2019).

The only preserved rostrum and orbital region elements in the holotype of *Undorosaurus gorodischensis* (UPM EP-II-20[572]) are a well preserved nasal, a parietal, and broken jugal and quadratojugal, that are barely overlapping with the preserved elements in PMO 214.578 (*Undorosaurus*? *kristiansenae*). The parietal is hard to interpret in PMO 214.578 as the skull is laterally compressed. The posterior portion of the nasals in *Undorosaurus gorodischensis* is not preserved, and the preserved portion is similar both to *Ophthalmosaurus icenicus* (Moon and Kirton 2016) and PMO 214.578. The quadratojugal fragment of UPM EP-II-20(572) has no features that are comparable to the well preserved element in PMO 214.578. The straight suborbital bar in the jugal fragment of UPM EP-II-20(572) resembles the complete element of PMO 214.578, but there is no contact between the jugal and the subnarial process of the premaxilla in PMO 214.578, contrary to the reconstruction by Zverkov and Efimov (2019: fig. 3C and SOM 3), even when the deformation is considered. A ventral exposure of the maxilla between the two elements is clearly visible in PMO 214.578 as in *Ophthalmosaurus icenicus* (Moon and Kirton 2016). In PMO 214.578, the sutures of the postorbital are easily observed and the element is surprisingly small compared to *Ophthalmosaurus incenicus* (Moon and Kirton 2016: fig. 4), and more similar to *Ichthyosaurus communis* and *Leptonectes moorei* (McGowan and Motani 2003: pl. 2, text-fig. 69). The large anterodorsal projection of the postorbital limiting the posterior margin of the orbit in most ichthyosaurs is not present. The element contributing to the posterodorsal part of the orbit is clearly continuing medially to the postorbital and is covered by it ventralmost, and might represent a projection of the postfrontal. The quadrate is covered by the quadratojugal and postorbital in PMO 214.578 and only partly visible and thus cannot be compared to the complete element in UPM EP-II-20(572).

The scapula of UPM EP-II-20(572) (Zverkov and Efimov 2019: fig. 9A, D, E) lacks the acromion process seen in PMO 214.578 (Druckenmiller et al. 2012: fig. 8). Only two clavicle fragments are preserved in UPM EP-II-20(572), and cannot be compared to the complete element in PMO 214.578. The humeri are superficially similar, but the trochanter dorsalis is more pointed and well pronounced in proximal view in PMO 214.578 than in UPM EP-II-20(572) (Zverkov and Efimov 2019: fig. 11B). The radius in UPM EP-II-20(572) is eroded and with a pentagonal shape, whereas it is polygonal

and anteroposteriorly wider than proximodirstally long in PMO 214.578 (Druckenmiller et al. 2012: fig. 9A–C). The radius and ulna of *Undorosaurus gorodischensis* are longer than wide in UPM EP-II-20(572) and YKM 44028-7 (Zverkov and Efimov 2019: fig. 11A, F). In this respect the holotype of *Undorosaurus nessovi* (UPM EP-II-24[785]) (Zverkov and Efimov 2019: fig. 17A) is more similar to PMO 214.578 than *Undorosaurus gorodischensis*.

Stratigraphic and geographic range.—Spitsbergen, Svalbard, Slottsmøya Member Lagerstätte, Tithonian.

Phylogenetic analysis

The most inclusive phylogenetic analysis (analysis 1) had a length of most parsimonious trees (MPT) of 326 steps (40 MPTs, CI = 0.37, RI = 0.66; Fig. 11A). When the most incomplete specimens were removed (analysis 2), tree length was 312 (30 MPTs, CI = 0.38, RI = 0.65; Fig. 11B). The strict consensus tree for Ophthalmosauridae for each analysis is given in Fig. 11 (for full tree see SOM 2.1). The resulting tree in analysis 2 is less resolved with a polytomy at the base of Ophthalmosauridae, and a majority rule tree (50%; Fig. 11C) is also shown, however with low ingroup support. A monophyletic Ophthalmosauridae was recovered, with *Stenopterygius aaleniensis* and *Chacaicosaurus cayi* as sister taxa. However, ingroup relationships in the family are poorly supported (Bremer support < 2), as in all previous studies (e.g., Fischer et al. 2016; Delsett et al. 2017). The resulting trees from the analyses without new characters (analysis 3 and 4) are shown in SOM 2.2.

Discussion

Taxonomic referral of the new specimens.—PMO 222.667 is referred to *Keilhauia* sp., a genus was described from the SML based on the early Berriasian holotype of *Keilhauia nui* (Delsett et al. 2017). The assignment is primarily based on a critical evaluation of skeletal similarities; and is consistent with its recovery as a sister taxon to the holotype specimen in the phylogenetic analysis. PMO 222.667 is not referred to the type species *Keilhauia nui* as there is no overlapping skull material, and the status of the autapomorphies in PMO 222.667 is unknown because the pelvic girdle and hindfin is not preserved. The two specimens can be scored for 20 overlapping phylogenetic characters in the postcranium, out of which they differ in only two. From the differential diagnosis of *Keilhauia nui*, PMO 222.667 shares a glenoid contribution of the scapula that is larger than the coracoid facet; a small dorsolateral flange of the scapula; an anteromedial process of coracoid; absence of a strongly developed deltopectoral crest of the humerus; a facet on the humerus for a preaxial accessory element anterior to radius, a posteriorly deflected ulnar facet on the humerus and a lack of contact
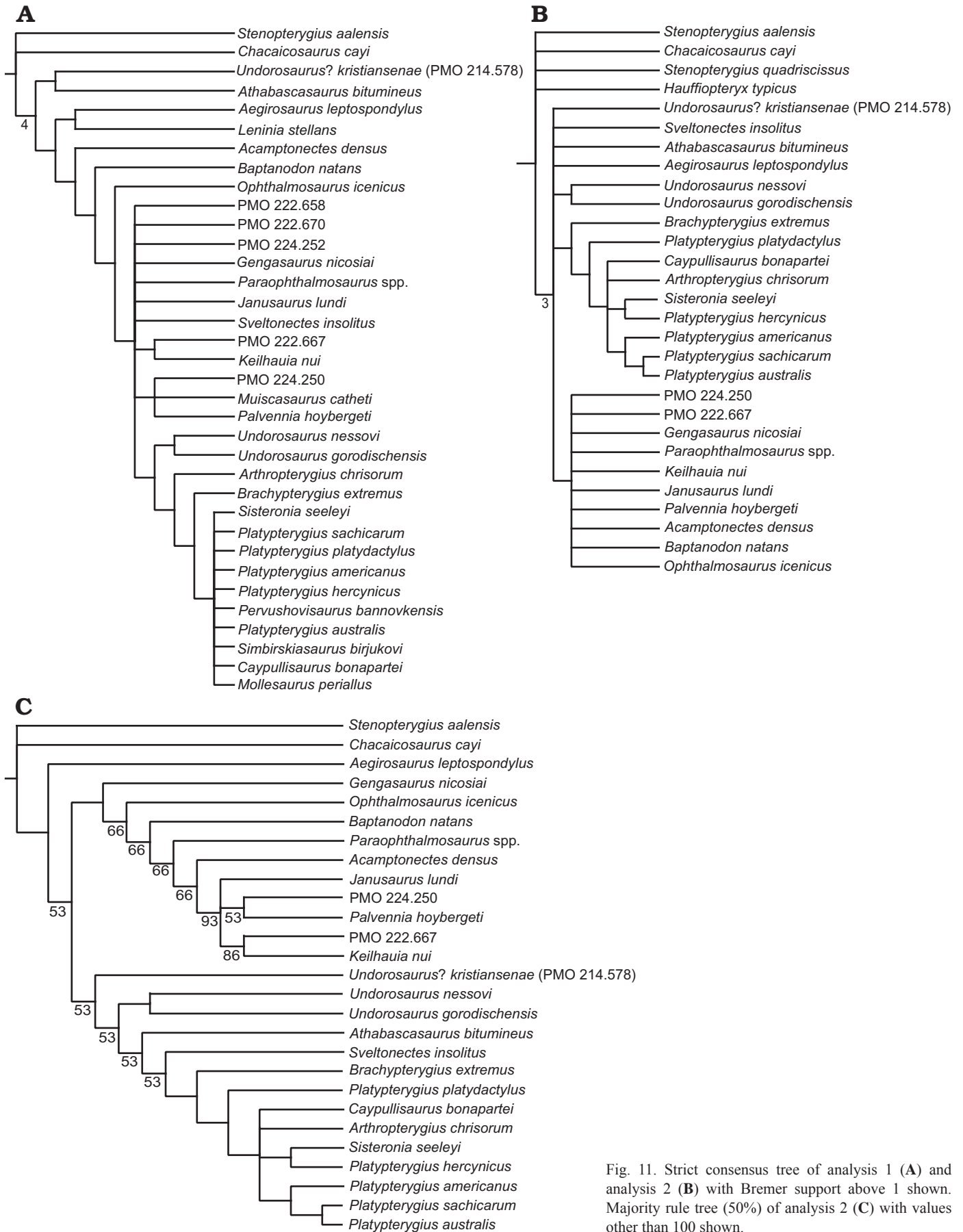
Fig. 11. Strict consensus tree of analysis 1 (**A**) and analysis 2 (**B**) with Bremer support above 1 shown. Majority rule tree (50%) of analysis 2 (**C**) with values other than 100 shown.

between the humerus and intermedium. PMO 222.667 also shares with *Keilhauia nui* an emarginated anterodorsal scapular margin, bicapitate ribs in the thoracic region, and rib facets are confluent with the anterior face in some centra. The coracoids have the same length: width ratio, an anterior notch and differs only in a less clear demarcation between the scapular and glenoid facet in PMO 222.667. In *Keilhauia nui* the radial facet on the humerus is slightly larger than the ulnar facet, while they are equally anteroposteriorly long in PMO 222.667; however, the difference is negligible and might result from intrageneric variation. The cross section of the ribs from the same region also differs; the holotype specimen of *Keilhauia nui* possesses the typical ophthalmosaurid figure of eight-shape while it is T-shaped in PMO 222.667. The stratigraphic difference between PMO 222.667 and the holotype of *Keilhauia nui* is large (equalling 10–12 million years), which argues against them belonging to a single species, but note that *Ophthalmosaurus icenicus* has a stratigraphic range that is much longer (Moon and Kirton 2016). The size difference might be ontogenetic, as the holotype of *Keilhauia nui* might be subadult (Delsett et al. 2017), or that they might represent two different species.

The new specimen shares with the SML ophthalmosaurids *Janusaurus lundi* and *Palvennia hoybergeti,* little or no extracondylar area visible in posterior view of the basioccipital, but differs from the two genera in approximately 25% of the overlapping phylogenetic characters. PMO 222.667 and *Janusaurus lundi* differ in the cross section of the ribs, coracoid length: width ratio, and the shape of the anterior margin of the anteromedial process of the coracoid. The unique morphology of the basisphenoid in PMO 222.667 differs from that in *Palvennia hoybergeti,* and they differ in the shape and size of the acromion process on the scapula (Roberts et al. 2014; Delsett et al. 2018).

PMO 224.252 is referred to Ophthalmosauridae indet. based on the large lateral exposure of the angular and the result of the phylogenetic result, where it is nested witihin Ophthalmosauridae (Fernández and Campos 2015; Moon 2017). The specimen lacks the orbital area, basicranium, vertebral column, fins and girdles, which makes a position within Ophthalmosauridae dubious. The specimen has more similarities with *Palvennia hoybergeti* and *Undorosaurus? kristiansenae* than with other SML taxa (Druckenmiller et al. 2012). The specimen does not possess the autapomorphies for these two species: the parietal foramen is small compared to the enlarged foramen in *Palvennia hoybergeti,* and the lacrimal does not have the 90° bend as in *Undorosaurus? kristiansenae.* It shares with *Undorosaurus? kristiansenae* the small supranarial process of the premaxilla, but differs in the curvature of the jugal and the cross section of the ribs. The slender rostrum with intermediate dentition differs from the more robust rostrum in *Keilhauia nui* and *Undorosaurus? kristiansenae,* and the morphology of the quadrate is different from *Palvennia hoybergeti* (Druckenmiller et al. 2012; Delsett et al. 2017).

Basicranium evolution.—Together, the specimens described herein provide new information on the ophthalmosaurid basicranium, which possesses taxonomically important characters, due in part to rapid evolution (Druckenmiller and Maxwell 2013; Arkhangelsky and Zverkov 2014; Fischer et al. 2014b; Fernández and Campos 2015). Previously it was believed that the other basicranial elements than the basioccipital were taxonomically uninformative, but subsequent work does not support this tenent (Fernández and Campos 2015). The basicranium of *Undorosaurus? kristiansenae* has more extracondylar area visible in posterior view than most ophthalmosaurids, partitioned into two peripheral rings that include the ventral surface. The *Keilhauia* sp. specimen PMO 222.667 has no extracondylar area visible in posterior view, and these two specimens represent the extremes with regard to amount of extracondylar area visible in posterior view. The amount of extracondylar area visible in posterior view is a feature that varies intraspecifically in *Ophthalmosaurus icenicus* (e.g., extensive exposure in NHMUK 4522 (personal observations AJR), little in OUMNH J12452 and LEIUG 90986 (personal observations LLD). This large variation in supposedly "ophthalmosaurinae" ophthalmosaurids might mean that this character cannot be used to distinguish the clades (Fischer et al. 2012; Fischer et al. 2014b) as is also suggested by work on *Platypterygius australis* (Kear and Zammit 2014). The *Keilhauia* sp. specimen PMO 222.667 has a unique basisphenoid as it does not possess basipterygoid processes, and a new phylogenetic character was incorporated to reflect this (character 95). Caution should be taken as basipterygoid process size might increase with age (Kear and Zammit 2014), but for PMO 222.667 the ontogeny is well established due to other features. It shares with *Arthropterygius chrisorum* and *Palvennia hoybergeti* a basisphenoid with anterior and posterior openings for the carotid artery, in contrast to other ophthalmosaurids where it enters and exits the element ventrally. In turtles, the evolution of the pattern of carotid circulation is complex because of the different ossification patterns of the para- and basisphenoid (Sterli et al. 2010), and this might be true also for ichthyosaurs.

***Undorosaurus* and *Cryopterygius*.**—*Cryopterygius kristiansenae* is known to differ from other SML specimens in a number of traits (Roberts et al. 2014; Maxwell et al. 2015; Fischer et al. 2016; Paparella et al. 2016; Delsett et al. 2017), and was recently synonymized with *Undorosaurus gorodischensis* (Zverkov and Efimov 2019). A second species of *Cryopterygius, Cryopterygius kielane,* was recently described from the Tithonian Owadów-Brzezinki Quarry in Poland (Tyborowski 2016). The holotype of *Undorosaurus* is UPM EP-II-20(572) and referred specimens are PMO 214.578 (holotype of *Cryopterygius kristiansenae*); UPM EP-II-23(744); UPM EP-II-21(1075); UPM EP-II-27(870) (holotype of *U. khorlovensis*) (Zverkov and Efimov 2019). We miss a formal statement on the reasons for referring other Russian specimens than the holotype to *Undorosaurus*

gorodischensis, given that the material is very incomplete. The paper (Zverkov and Efimov 2019) in some paragraphs assigns UPM EP-II-22(1073) and YKM 44028-7 to *U. gorodischensis*, whereas in other to *Undorosaurus* sp.

The new diagnosis of *Undorosaurus gorodischensis* by Zverkov and Efimov (2019) is a unique character combination relative to other species of *Undorosaurus* with ten characters. Out of these, only three, and possibly a fourth, are true for both PMO 214.578 and the holotype of *U. gorodischensis*: extensive anterolaterally directed basipterygoid processes of the basisphenoid; slightly pronounced anterodistal accessory facet of the humerus, and small pisiform facet of the ulna. Possibly also an ulna posterior edge proximodistally elongate and not involved in perichondral ossification. All of these characters are shared by at least one other ophthalmosaurid taxa, and thus not sufficient for referring these specimens to the same species. For two characters, the Russian *Undorosaurus* specimens and PMO 214.578 actually differ: teardrop-shaped stapedial head in medial view, that points dorsally, and a humerus with extensive and anteroposteriorly elongate proximal end, poorly pronounced trochanter dorsalis and deltopectoral crest. The stapes is teardrop-shaped in the *Undorosaurus gorodischensis* holotype, but not in PMO 214.578 (oval), poorly preserved in UPM EP-II-23(744) and not pictured for UPM EP-II-22(1073). The proximal end of the humerus in the *Undorosaurus gorodischensis* holotype differs from PMO 214.578, and is instead more similar to UPM EP-II-23(744). Thirdly, three characters in the diagnosis cannot be observed in PMO 214.578 at all, due to preservation: a quadrate with relatively mediolaterally compressed condyle (only in the *Undorosaurus gorodischensis* holotype and UPM EP-II-22(1073)); articular isometric in medial view, without medial bulge; (only in the *Undorosaurus gorodischensis* holotype), and humerus length to quadrate height ratio 1.01 (can only be calculated for UPM EP-II-20[572]). One character; relatively small forelimb (humerus to jaw length ratio c. 0.112) cannot be observed in any of the Russian *Undorosaurus* specimens, and only in PMO 214.578 because it is the only specimen with a preserved lower jaw.

In total, we find that the diagnosis of *Undorosaurus gorodischensis* is not covering the specimens currently assigned to the species, partly due to a number of misinterpretations as shown above, and partly due to the lack of overlap between the Russian specimens and PMO 214.578. Our phylogenetic analysis does also not support a common species. *Undorosaurus*? *kristiansenae* is not recovered in a monophyletic clade with the other *Undorosaurus* species, and based on the re-examination herein where several misinterpretations and differences were discovered, we disagree with the statement that there is not "any feature in overlapping material that could be used to distinguish *Undorosaurus*? *kristiansenae* as a valid species of *Undorosaurus*" (Zverkov and Efimov 2019). However, there are clearly many similarities between the specimens previously assigned to *Cryopterygius* and *Undorosaurus* in

the basicranium (this contribution) and the fore- and hindfins (Druckenmiller et al. 2012; Arkhangelsky and Zverkov 2014; Delsett et al. 2017, 2018). The ischiopubis is also similar and might have taxonomic significance (Delsett et al. 2017; Zverkov and Efimov 2019). For now, we refer PMO 214.578 to *Undorosaurus*? *kristiansenae*. A new diagnosis for *Undorosaurus* and *U. gorodischensis* is needed, as well as a continued work to expand the dataset used for phylogenetic analysis of ophthalmosaurids.

Synonymy of SML taxa to *Arthropterygius*.—Zverkov and Prilepskaya (2019) argue that *Keilhauia nui, Janusaurus lundi* and *Palvennia hoybergeti* can be referred to *Arthropterygius*. A full evaluation of this hypothesis will be the topic of a follow-up paper, but some major points are addressed here. We cannot accept the synonymy as presented in Zverkov and Prilepskaya (2019), because we find several problematic issues with their arguments. A major point is that different skeletal parts are weighted differently through the discussion on taxonomic referral. Three characters on the humerus are said to "help for easy recrognition og humeri belongning to *Arthropterygius* among those of other ophthalmosaurids" (Zverkov and Prilepskaya 2019: 2). Ichthyosaur humeri are frequently preserved and are important for taxonomy, but they alone are not sufficient for referring a specimen to a genus. In Zverkov and Prilepskaya (2019) a PCA is conducted on a number of traits on the humerus. The variation between the left and right humeri is for some specimens (Zverkov and Prilepskaya: fig. 20) larger than the variation within some of the genera. This is explained in the paper with asymmetry in ophthalmosaurids, but it shows that caution should be taken in using humeri for taxonomic referral.

The two remarkably similar specimens of *Palvennia hoybergeti* (Delsett et al. 2018) are viewed to belong to different species (Zverkov and Prilepskaya 2019). An enlarged parietal foramen is an autapomorphy of *Palvennia hoybergeti* (Druckenmiller et al. 2012; Delsett et al. 2018), and we disagree with Zverkov and Prilepskaya's (2019) interpretation that such a structure is present in the holotype of *Janusaurus lundi,* as the skull roof is totally crushed into small skeletal fragments (Roberts et al. 2014). Many ophthalmosaurid taxa do not preserve a complete and articulated skull roof, and thus this feature might of course be more widespread than is known at the moment. This is however always the case with incomplete specimens, and the feature should be treated as an autapomorphy until proven otherwise. Zverkov and Prilepskaya (2019) also use their interpretation of the humerus and clavicle remains from the holotype of *Palvennia hoybergeti* (SVB 1451). These elements are highly incomplete, and the clavicle is severly distorted. Both represent too uncertain data points for inclusion in a taxonomic argument. Differences between *Palvennia hoybergeti* and *Arthropterygius chrisorum* (Delsett et al. 2018) are in Zverkov and Prilepskaya (2019) seen as neglible as "none of these differences are sufficient enough" or that "this could be explained by ontogenetic variation" (Zverkov

and Prilepskaya 2019: 51), which in our opinion are not well-supported claims.

As stated in the original description of the the holotype of *Keilhauia nui* (Delsett et al. 2017), the preservation of the holotype specimen (PMO 222.655) is relatively poor and there is some uncertainty regarding its ontogenetic status. Zverkov and Prilepskaya (2019) consider it a nomen dubium, and it is removed from the phylogenetic analysis, "considered undiagnostic". This becomes highly problematic when the very same skeletal elements are used for referring the specimen to *Arthropterygius* (in open nomenclature), are used as support for four characters in the diagnosis for the genus, and also in the reconstrucion of the ontogenetic trajectory of *Arthropterygius* (Zverkov and Prilepskaya 2019).

Phylogenetic analysis.—The resulting trees from our analysis vary largely, and it is evident that phylogenetic analysis of ophthalmosaurids still is very vulnerable to which characters and OTUs are included, and caution should be taken when interpreting the results. The low number of largely complete and articulated ophthalmosaurids, as well as many taxa based solely on cranial material pose challenges for phylogenetic analysis, as do possible convergent evolution (Maxwell et al. 2015; Moon 2017; Massare and Lomax 2018).

A clade relatively similar to Platypterygiinae sensu Fischer et al. (2016) is recovered based on the largest dataset (analysis 1), excluding *Aegirosaurus leptospondylus*, *Sveltonectes insolitus*, and *Athabascasaurus bitumineus* that are in some studies nested within this group (Fischer et al. 2016; but see Roberts et al. 2014; Maxwell et al. 2015). *Arthropterygius chrisorum*, *Undorosaurus gorodischensis*, and *U. nessovi* are recovered as succesive sister taxa. No monophyletic Ophthalmosaurinae is recovered, in contrast to some previous studies (e.g., Fischer et al. 2016; Delsett et al. 2017) but similar to others (Maxwell et al. 2015).

When incomplete OTUs are removed (analysis 2), a monophyletic Platypterygiinae, excluding *Aegirosaurus leptospondylus,* is found in 53% of the trees (Fig. 11C), with the three *Undorosaurus* species as succesive sister taxa to the clade, while they in two previous studies (Zverkov and Efimov 2019; Zverkov and Prilepskaya 2019) are nested within Platypterygiinae. An "ophthalmosaurinae" clade sensu Fischer et al. 2016 is found in all trees. All of the SML specimens, with the notable exception of *Undorosaurus*? *kristiansenae*, form a monophyletic group within "Ophthalmosaurinae". PMO 222.667 and *Keilhauia nui* form a clade in 86% of the trees in analysis 2, and also among the otherwise unresolved non-platypterygiine species in analysis 1. Compared to previous analyses that found *Keilhauia nui* as basal within Ophthalmosauridae (Delsett et al. 2017) or as a sister taxon to *Platypterygius* species (Moon 2017), the position of it is relatively stable in the present study, possibly as a result of being scored for a larger number of postcranial characters.

When the new characters (mainly postcranial) are excluded (analysis 3 and 4) the resulting tree is more similar to Fischer et al. (2016) in showing two monophyletic clades. *Arthriopterygius chrisorum* occupies a basal position in the family, similar to several other analyses (Roberts et al. 2014; Fischer et al. 2016), but in contrast to a position together with the SML taxa (Maxwell et al. 2015) and to the result in analysis 1 and 2. A plausible reason for this unstable placement is the lack of almost any cranial material in the holotype. In the phylogenetic analysis of Zverkov and Prilepskaya (2019), an unusually well-supported clade of four *Arthropterygius* species, including all SML specimens except for PMO 214.578 (*Undorosaurus*? *kristiansenae*) is found (Bremer support 5 or 4, depending on which taxa are included). Compared to our analysis, the two character matrices differ in very many aspects even though both build on the dataset by Fischer et al. (2016) of 88 characters to a larger or smaller degree. A total of 13 characters are modified, 19 removed and 43 characters added in Zverkov and Prilepskaya (2019), based on Zverkov and Efimov (2019), and a number of specimens are rescored for several characters. A full comparison of the results is thus beyond the scope of this paper.

Conclusions

Slottsmøya Member Lagerstätte is one of the richest localities for Late Jurassic–Early Cretaceous ichthyosaurs (Hurum et al. 2012). Through eight field seasons (2004–2012), 26 ichthyosaur specimens were excavated and out of these are twelve formally described in this contribution and previous papers (Druckenmiller et al. 2012; Roberts et al. 2014; Delsett et al. 2017, 2018). Through this contribution, a second *Keilhauia* specimen, a large Ophthalmosauridae indet. skull and new material from *Undorosaurus*? *kristiansenae* has been described, adding to the knowledge on the skull and especially the basicranium in the group. This is also the first phylogenetic analysis including all the SML specimens. The SML specimens provide valuable data points for the understanding of ophthalmosaurid phylogeny and evolution as well as the palaeobiogeography, but also shows that our understanding of ichthyosaur phylogeny and biogeography is still incomplete. Articulated and complete specimens, and specimens that can provide additional postcranial information, are needed to solve these questions.

Acknowledgments

References

Arkhangelsky, M.S. 1997. On a new ichthyosaurian genus from the Lower Volgian Substage of the Saratov, Volga region. *Paleontological Journal* 31: 87–90.

Arkhangelsky, M.S. and Zverkov, N.G. 2014. On a new ichthyosaur of the genus *Undorosaurus*. *Proceedings of the Zoological Institute RAS* 318: 187–196.

Arkhangelsky, M.S., Zverkov, N.G., Spasskaya, O.S., and Evgrafov, A.V. 2018. On the first reliable record of the ichthyosaur *Ophthalmosaurus icenicus* Seeley in the Oxfordian–Kimmeridgian beds of European Russia. *Paleontological Journal* 52: 49–57.

Bardet, N. and Fernández, M. 2000. A new ichthyosaur from the Upper Jurassic lithographic limestones of Bavaria. *Journal of Paleontology* 74: 503–511.

Baur, G. 1887. On the morphology and origin of the Ichthyopterygia. *American Naturalist* 21: 837–840.

Boulenger, G.A. 1904. Exhibition of, and remarks upon, a paddle of a new species of ichthyosaur. *Proceedings of the Zoological Society of London* 1: 424–426.

Buchholtz, E.A. 2001. Swimming styles in Jurassic ichthyosaurs. *Journal of Vertebrate Paleontology* 21: 61–73.

Collignon, M. and Hammer, Ø. 2012. Petrography and sedimentology of the Slottsmøya Member at Janusfjellet, central Spitsbergen. *Norwegian Journal of Geology* 92: 89–101.

de Blainville, M.H.D. 1835. Description de quelques espèces de reptiles de la Californie, précédée de l'analyse d'un systéme général d'erpétologie et d'amphibiologie *Nouvelles annales du muséum d'histoire naturelle* 4: 233–296.

Delsett, L.L., Druckenmiller, P.S., Roberts, A.J., and Hurum, J.H. 2018. A new specimen of *Palvennia hoybergeti*: Implications for cranial and pectoral girdle anatomy in ophthalmosaurid ichthyosaurs. *PeerJ* e5776.

Delsett, L.L., Novis, L.K., Roberts, A.J., Koevoets, M.J., Hammer, Ø., Druckenmiller, P.S., and Hurum, J.H. 2016. The Slottsmøya marine reptile Lagerstätte: depositional environments, taphonomy and diagenesis. *Geological Society Special Publications: Mesozoic Biotas of Scandinavia and its Arctic Territories* 434: 165–188.

Delsett, L.L., Roberts, A.J., Druckenmiller, P.S., and Hurum, J.H. 2017. A new ophthalmosaurid (Ichthyosauria) from Svalbard, Norway, and evolution of the ichthyopterygian pelvic girdle. *PLoS ONE* 12 (1): e0169971.

Druckenmiller, P.S. and Maxwell, E.E. 2010. A new Lower Cretaceous (lower Albian) ichthyosaur genus from the Clearwater Formation, Alberta, Canada. *Canadian Journal of Earth Sciences* 47: 1037–1053.

Druckenmiller, P.S. and Maxwell, E.E. 2013. A Middle Jurassic (Bajocian) ophthalmosaurid (Reptilia, Ichthyosauria) from the Tuxedni Formation, Alaska and the early diversification of the clade. *Geological Magazine* 151: 41–48.

Druckenmiller, P.S., Hurum, J.H., Knutsen, E.M., and Nakrem, H.A. 2012. Two new ophthalmosaurids (Reptilia: Ichthyosauria) from the Agardhfjellet Formation (Upper Jurassic: Volgian/Tithonian), Svalbard, Norway. *Norwegian Journal of Geology* 92: 311–339.

Dypvik, H. and Zakharov, V. 2012. Fine-grained epicontinental Arctic sedimentation—mineralogy and geochemistry of shales from the Late Jurassic–Early Cretaceous transition. *Norwegian Journal of Geology* 92: 65–87.

Efimov, V.M. 1997. *Undorosaurus* [in Russian]. 208 pp. Ph.D. thesis, Saratov University, Saratov.

Efimov, V.M. 1999a. A new family of ichthyosaurs, the Undorosauridae fam. nov. from the Volgian Stage of the European part of Russia. *Paleontological Journal* 33: 174–181.

Efimov, V.M. 1999b. Ichthyosaurs of a new genus *Yasykovia* from the Upper Jurassic Strata of European Russia. *Paleontological Journal* 33: 91–98.

Fernández, M.S. 1999. A new ichthyosaur from the Los Molles Formation (Early Bajocian), Neuquen Basin, Argentina. *Journal of Paleontology* 73: 677–681.

Fernández, M. 2007. Redescription and phylogenetic position of *Caypullisaurus* (Ichthyosauria: Ophthalmosauridae). *Journal of Paleontology* 81: 368–375.

Fernández, M.S. and Campos, L. 2015. Ophthalmosaurids (Ichthyosauria: Thunnosauria): Alpha taxonomy, clades and names. *Publicación Electrónica de la Asociación Paleontológica Argentina* 15: 20–30.

Fernández, M.S. and Talevi, M. 2014. Ophthalmosaurian (Ichthyosauria) records from the Aalenian–Bajocian of Patagonia (Argentina): an overview. *Geological Magazine* 151: 49–59.

Fernández, M.S., Vennari, V.V., Herrera, Y., Campos, L., Talevi, M., and de la Fuente, M. 2018. New marine reptile assemblage from the Jurassic–Cretaceous boundary beds of the High Andes, Argentina. *In*: C.R. Domínguez and F. Olóriz (eds.), *10th International Congress on the Jurassic System. Abstracts*, 52–55. Paleontología Mexicana, Universidad Nacional Autónoma de México, Mexico.

Fischer, V. 2012. New data on the ichthyosaur *Platypterygius hercynicus* and its implications for the validity of the genus. *Acta Palaeontologica Polonica* 57: 123–134.

Fischer, V. 2016. Taxonomy of *Platypterygius campylodon* and the diversity of the last ichthyosaurs. *PeerJ* 4: e2604.

Fischer, V., Appleby, R.M., Naish, D., Liston, J., Riding, J.B., Brindley, S., and Godefroit, P. 2013a. A basal thunnosaurian from Iraq reveals disparate phylogenetic origins for Cretaceous ichthyosaurs. *Biology Letters* 9 (4): 1–6.

Fischer, V., Arkhangelsky, M.S., Naish, D., Stenshin, I.M., Uspensky, G.N., and Godefroit, P. 2014b. *Simbirskiasaurus* and *Pervushovisaurus* reassessed: implications for the taxonomy and cranial osteology of Cretaceous platypterygiine ichthyosaurs. *Zoological Journal of the Linnean Society* 171: 822–841.

Fischer, V., Arkhangelsky, M.S., Uspensky, G.N., Stenshin, I.M., and Godefroit, P. 2013b. A new Lower Cretaceous ichthyosaur from Russia reveals skull shape conservatism within Ophthalmosaurinae. *Geological Magazine* 151: 60–70.

Fischer, V., Bardet, N., Benson, R.B.J., Arkhangelsky, M.S., and Friedman, M. 2016. Extinction of fish-shaped marine reptiles associated with reduced evolutionary rates and global environmental volatility. *Nature Communications* 7: 10825.

Fischer, V., Bardet, N., Guiomar, M., and Godefroit, P. 2014a. High diversity in Cretaceous ichthyosaurs from Europe prior to their extinction. *PLoS ONE* 9 (1): e84709.

Fischer, V., Maisch, M.W., Naish, D., Kosma, R., Liston, J., Joger, U., Krüger, F.J., Pardo-Pérez, J.M., Tainsh, J., and Appleby, R.M. 2012. New ophthalmosaurid ichthyosaurs from the European Lower Cretaceous demonstrate extensive ichthyosaur survival across the Jurassic–Cretaceous boundary. *PLoS ONE* 7 (1): e29234.

Fischer, V., Masure, E., Arkhangelsky, M.S., and Godefroit, P. 2011. A new Barremian (Early Cretaceous) ichthyosaur from Western Russia. *Journal of Vertebrate Paleontology* 31: 1010–1025.

Gilmore, C.W. 1906. Notes on osteology of *Baptanodon*. With a description of a new species. *Memoirs of the Carnegie Museum* 2 (9): 325–342.

Goloboff, F. and Catalano, S. 2016. TNT, version 1.5, with a full implementation of phylogenetic morphometrics. *Cladistics* 32: 221–238.

Hammer, Ø., Collignon, M., and Nakrem, H.A. 2012. Organic carbon isotope chemostratigraphy and cyclostratigraphy in the Volgian of Svalbard. *Norwegian Journal of Geology* 92: 103–112.

Hryniewicz, K., Nakrem, H.A., Hammer, Ø., Little, C.T.S., Kaim, A., Sandy, M.R., and Hurum, J.H. 2015. The palaeoecology of the latest Jurassic–earliest Cretaceous hydrocarbon seep carbonates from Spitsbergen, Svalbard. *Lethaia* 48: 353–374.

Hulke, J.W. 1871. Note on an *Ichthyosaurus* (*I. enthekiodon*) from Kimmeridge Bay, Dorset. *Quarterly Journal of the Geological Society* 27: 440–441.

Hurum, J.H., Nakrem, H.A., Hammer, Ø., Knutsen, E.M., Druckenmiller, P.S., Hryniewicz, K., and Novis, L.K. 2012. An Arctic Lagerstätte—the Slottsmøya Member of the Agardhfjellet Formation (Upper Jurassic–Lower Cretaceous) of Spitsbergen. *Norwegian Journal of Geology* 92: 55–64.

Johnson, R. 1977. Size independent criteria for estimating age and the relationships among growth parameters in a group of fossil reptiles (Reptilia: Ichthyosauria). *Canadian Journal of Earth Sciences* 14 (8): 1916–1924.

Kear, B.P. 2005. Cranial morphology of *Platypterygius longmani* Wade, 1990 (Reptilia: Ichthyosauria) from the Lower Cretaceous of Australia. *Zoological Journal of the Linnean Society* 145 (4): 583–622.

Kear, B.P. and Zammit, M. 2014. *In utero* foetal remains of the Cretaceous ichthyosaurian *Platypterygius*: ontogenetic implications for character state efficacy. *Geological Magazine* 151 (1): 71–86.

Kirton, A.M. 1983. *A Review of British Upper Jurassic Ichthyosaurs*. 366 pp. Unpublished Ph.D. Thesis, University of Newcastle upon Tyne, Newcastle upon Tyne.

Koevoets, M.J. 2017. *The Palaeontology, Stratigraphy and Palaeo-environment of the Agardhfjellet Formation (Middle Jurassic–Lowermost Cretaceous) of Spitsbergen, Svalbard*. 190 pp. University of Oslo, Oslo.

Koevoets, M.J., Abay, T.B., Hammer, Ø., and Olaussen, S. 2016. High-resolution organic carbon-isotope stratigraphy of the Middle Jurassic–Lower Cretaceous Agardhfjellet Formation of central Spitsbergen, Svalbard. *Palaeogeography, Palaeoclimatology, Palaeoecology* 449: 266–274.

Koevoets, M.J., Hammer, Ø., Olaussen, S., Senger, K., and Smelror, M. 2018. Integrating subsurface and outcrop data of the Middle Jurassic to Lower Cretaceous Agardhfjellet Formation in central Spitsbergen. *Norwegian Journal of Geology* 98: 1–34.

Kolb, C. and Sander, P.M. 2009. Redescription of the ichthyosaur *Platypterygius hercynicus* (Kuhn 1946) from the Lower Cretaceous of Salzgitter (Lower Saxony, Germany). *Palaeontographica Abteilung A: Paläozoologie-Stratigraphie* 288: 151–192.

Maisch, M.W. 2010. Phylogeny, systematics, and origin of the Ichthyosauria—the state of the art. *Palaeodiversity* 3: 151–214.

Maisch, M.W. and Matzke, A.T. 2000. The Ichthyosauria. *Stuttgarter Beiträge zur Naturkunde Serie B* 298: 1–159.

Massare, J.A. and Lomax, D.R. 2018. Hindfins of *Ichthyosaurus*: effects of large sample size on "distinct" morphological characters. *Geological Magazine* 156: 1–20.

Maxwell, E.E. 2010. Generic reassignment of an ichthyosaur from the Queen Elizabeth Islands, Northwest Territories, Canada. *Journal of Vertebrate Paleontology* 30: 403–415.

Maxwell, E.E. and Caldwell, M.W. 2006. A new genus of ichthyosaur from the Lower Cretaceous of Western Canada. *Palaeontology* 49 (5): 1043–1052.

Maxwell, E.E. and Kear, B.P. 2010. Postcranial anatomy of *Platypterygius americanus* (Reptilia: Ichthyosauria) from the Cretaceous of Wyoming. *Journal of Vertebrate Paleontology* 30 (4): 1059–1068.

Maxwell, E.E., Dick, D., Padilla, S., and Parra, M.L. 2015. A new ophthalmosaurid ichthyosaur from the Early Cretaceous of Colombia. *Papers in Palaeontology* 2 (1): 59–70.

McGowan, C. 1972. The systematics of Cretaceous ichthyosaurs with particular reference to the material from North America. *Contributions to Geology* 11 (1): 9–29.

McGowan, C. 1976. Description and phenetic relationships of a new ichthyosaur genus from the Upper Jurassic of England. *Canadian Journal of Earth Sciences* 13: 668–683.

McGowan, C. and Motani, R. 2003. *Ichthyopterygia*. 182 pp. Verlag Dr. Friedrich Pfeil, München.

Moon, B.C. and Kirton, A.M. 2016. Ichthyosaurs of the British Middle and Upper Jurassic. Part 1 *Ophthalmosaurus*. *Monograph of the Palaeontographical Society* 170: 1–84.

Moon, B.C. 2017. A new phylogeny of ichthyosaurs (Reptilia: Diapsida). *Journal of Systematic Palaeontology* 17: 129–155.

Motani, R. 1999. Phylogeny of the Ichthyopterygia. *Journal of Vertebrate Paleontology* 19: 473–496.

Mutterlose, J., Brumsack, H., Flögel, S., Hay, W., Klein, C., Langrock, U., Lipinski, M., Ricken, W., Söding, E., Stein, R., and Swientek, O. 2003. The Greenland-Norwegian Seaway: A key for understanding Late Jurassic to Early Cretaceous paleoenvironments. *Paleoceanography* 18: 1–26.

Paparella, I., Maxwell, E.E., Cipriani, A., Roncacè, S., and Caldwell, M.W. 2016. The first ophthalmosaurid ichthyosaur from the Upper Jurassic of the Umbrian–Marchean Apennines (Marche, Central Italy). *Geological Magazine* 154: 837–858.

Roberts, A.J., Druckenmiller, P.S., Sætre, G.-P., and Hurum, J.H. 2014. A New Upper Jurassic Ophthalmosaurid Ichthyosaur from the Slottsmøya Member, Agardhfjellet Formation of Central Spitsbergen. *PLoS ONE* 9 (8): e103152.

Roberts, A.J., Funke, M.L.K., Engelschiøn, V.S., and Hurum, J.H. 2019. The Excavation of high Arctic, Late Jurassic–Early Cretaceous marine reptiles and their virtual and manual preparation. *Geological Curator* 11: 69–80.

Rousseau, J. and Nakrem, H.A. 2012. An Upper Jurassic Boreal echinoderm Lagerstätte from Janusfjellet, central Spitsbergen. *Norwegian Journal of Geology* 92: 133–148.

Rousseau, J., Gale, A.S., and Thuy, B. 2018. New articulated asteroids (Echinodermata, Asteroidea) and ophiuroids (Echinodermata, Ophiuroidea) from the Late Jurassic (Volgian/Tithonian) of central Spitsbergen. *European Journal of Taxonomy* 411: 1–26.

Sander, P.M. 2000. Ichthyosauria: their diversity, distribution, and phylogeny. *Paläontologische Zeitschrift* 74: 1–35.

Sterli, J., Müller, J., Anquetin, J., and Hilger, A. 2010. The parabasisphenoid complex in Mesozoic turtles and the evolution of the testudinate basicranium. *Canadian Journal of Earth Sciences* 47: 1337–1346.

Storrs, G.W., Arkhangelsky, M.S., and Efimov, V.M. 2000. Mesozoic marine reptiles of Russia and other former Soviet republics. *In*: M.J. Benton, M.A. Shishkin, D.M. Unwin, and E. Kurochkin (eds.), *The Age of Dinosaurs in Russia and Mongolia*, 187–209. Cambridge University Press, Cambridge.

Torsvik, T.H. van der, Voo, R., Preeden, U., Mac Niocaill, C., Steinberger, B., Doubrovine, P.V., Hinsbergen, D.J.J. van, Domeier, M., Gaina, C., Tohver, E., Meert, J.G., McCausland, P.J.A., and Cocks, L.R.M. 2012. Phanerozoic polar wander, palaeogeography and dynamics. *Earth-Science Reviews* 114: 325–368.

Tyborowski, D. 2016. A new ophthalmosaurid ichthyosaur from the Late Jurassic of Owadów-Brzezinki Quarry, Poland. *Acta Palaeontologica Polonica* 61: 791–803.

Zammit, M., Norris, R.M., and Kear, B.P. 2010. The Australian Cretaceous ichthyosaur *Platypterygius australis*: A description and review of postcranial remains. *Journal of Vertebrate Paleontology* 30: 1726–1735.

Zverkov, N.G. and Efimov, V.M. 2019. Revision of Undorosaurus, a mysterious Late Jurassic ichthyosaur of the Boreal Realm. *Journal of Systematic Palaeontology* 17: 1183–1213.

Zverkov, N.G. and Prilepskaya, N.E. 2019. A prevalence of Arthropterygius (Ichthyosauria: Ophthalmosauridae) in the Late Jurassic–earliest Cretaceous of the Boreal Realm. *PeerJ* 7: e6799.

Zverkov, N.G., Arkhangelsky, M.S., and Stenshin, I.M. 2015a. A review of Russian Upper Jurassic Ichthyosaurs with an intermedium/humeral contact. Reassessing *Grendelius* McGowan, 1976. *Proceeding of the Zoological Institute RAS* 319: 558–588.

Zverkov, N.G., Arkhangelsky, M.S., Pardo-Pérez, J., and Beznosov, P.A. 2015b. On the Upper Jurassic ichthyosaur remains from the Russian North. *Proceedings of the Zoological Institute RAS* 319: 81–97.